surrogate markers for atherosclerosis.

The necessity for thyroid hormone replacements therapy for SCH is not supported by the present study results. The signs and symptoms of hypothyroidism are bradycardia, mild hypertension and hyperlipidemia, which might accelerate atherosclerosis in subjects with hypothyroidism.[16] We examined the association between SCH and these symptoms or signs and did not observe an association between SCH and blood pressure or serum lipid levels. The association between lipid profile and SCH has been previously reported in Norway and Australia[6,7] and the different results might relate to differences in genetic background, life style and BMI. In the Tromsø study[7] the subjects were obese and those with SCH were even more obese than normal subjects. The difference in BMI between those and our investigations might induce different patterns of lipid metabolism. We did not observe any significant association between SCH and the symptoms or signs associated with hypothyroidism. Moreover, we did not find an association between SCH and IMT, as a surrogate marker for atherosclerosis, and did not find an association between SCN and past history of atherosclerotic disease. These results do not support the need for treatment of SCH in Japanese subjects. However, our investigation was a cross-sectional study, so the duration of SCH was not considered in the analysis. Our results do not completely deny that subjects with long-term SCH have increased risk of atherosclerosis.

In conclusion, we examined the association between subclinical thyroid dysfunction and various factors in a general population. We only found an association between glucose levels and subclinical thyroid dysfunction. The differences in serum glucose levels among the thyroid states (SCH, subclinical hyperthyroidism, and normal thyroid) were too small to lead to a recommendation for treatment of subclinical thyroid dysfunction and thus do not indicate a need for treatment of subclinical thyroid dysfunction in Japanese subjects.

Acknowledgements

This study was supported by a grant from the Program for Promotion of Fundamental Studies in Health Science of the National Institute of Biomedical Innovation. We acknowledge the contribution of the members of this study.

References

1. Canaris GJ, Manowitz NR, Mayor G, Ridgway EC. The Colorado thyroid disease prevalence study. *Arch Intern Med* 2000; **160:** 526–534.
2. Gharib H, Tuttle RM, Baskin HJ, Fish LH, Singer PA, McDermott MT. Subclinical thyroid dysfunction: A joint statement on management from the American Association of Clinical Endocrinologists, the American Thyroid Association, and the Endocrine Society. *J Clin Endocrinol Metab* 2005; **90:** 581–585; discussion 586–587.
3. Sawin CT, Castelli WP, Hershman JM, McNamara P, Bacharach P. The aging thyroid: Thyroid deficiency in the Framingham Study. *Arch Intern Med* 1985; **145:** 1386–1388.
4. Samuels MH. Subclinical thyroid disease in the elderly. *Thyroid* 1998; **8:** 803–813.
5. Hueston WJ, Pearson WS. Subclinical hypothyroidism and the risk of hypercholesterolemia. *Ann Fam Med* 2004; **2:** 351–355.
6. Walsh JP, Bremner AP, Bulsara MK, O'Leary P, Leedman PJ, Feddema P, et al. Thyroid dysfunction and serum lipids: A community-based study. *Clin Endocrinol (Oxf)* 2005; **63:** 670–675.
7. Iqbal A, Jorde R, Figenschau Y. Serum lipid levels in relation to serum thyroid stimulating hormone and the effect of thyroxine treatment on serum lipid levels 7 in subjects with subclinical hypothyroidism: The Tromso Study. *J Intern Med* 2006; **260:** 53–61.
8. Biondi B, Palmieri EA, Lombardi G, Fazio S. Effects of subclinical thyroid dysfunction on the heart. *Ann Intern Med* 2002; **137:** 904–914.
9. Dagre AG, Lekakis JP, Papaioannou TG, Papamichael CM, Koutras DA, Stamatelopoulos SF, et al. Arterial stiffness is increased in subjects with hypothyroidism. *Int J Cardiol* 2005; **103:** 1–6.
10. Biondi B, Klein I. Hypothyroidism as a risk factor for cardiovascular disease. *Endocrine* 2004; **24:** 1–13.
11. Mannami T, Konishi M, Baba S, Nishi N, Terao A. Prevalence of asymptomatic carotid atherosclerotic lesions detected by high-resolution ultrasonography and its relation to cardiovascular risk factors in the general population of a Japanese city: The Suita study. *Stroke* 1997; **28:** 518–525.
12. Iwai N, Katsuya T, Mannami T, Higaki J, Ogihara T, Kokame K, et al. Association between SAH, an acyl-CoA synthetase gene, and hypertriglyceridemia, obesity, and hypertension. *Circulation* 2002; **105:** 41–47.
13. Kokubo Y, Iwai N, Tago N, Inamoto N, Okayama A, Yamawaki H, et al. Association analysis between hypertension and CYBA, CLCNKB, and KCNMB1 functional polymorphisms in the Japanese population: The Suita Study. *Circ J* 2005; **69:** 138–142.
14. Surks MI, Ortiz E, Daniels GH, Sawin CT, Col NF, Cobin RH, et al. Subclinical thyroid disease: Scientific review and guidelines for diagnosis and management. *JAMA* 2004; **291:** 228–238.
15. Dillmann WH. The thyroid. *In*: Bennett JC, editor. Cecil textbook of medicine, 20th edn. Philadelphia: WB Saunders; 1996; 1227–1245.
16. Irwin K, Kaie O. Thyroid hormone and the cardiovascular system. *N Engl J Med* 2001; **344:** 501–509.

Circ J 2007; **71:** 437–444

Nanomaterials Induce Oxidized Low-Density Lipoprotein Cellular Uptake in Macrophages and Platelet Aggregation

Yasuharu Niwa, PhD; Naoharu Iwai, MD

Background Nanomaterials have numerous potential benefits for society, but the potential hazards of nanomaterials on human health are poorly understood. Nanomaterials are known to pass into the circulatory system in humans, causing vascular injuries that might play a role in the development of atherosclerosis. The present study aimed to determine the effects of chronic exposure to nanomaterials on macrophage phenotype and platelet aggregation.

Methods and Results Cultured macrophages (RAW264.7) were treated with carbon black (CB) and water-soluble fullerene ($C_{60}(OH)_{24}$) from 7 to 50 days. Individually, CB had no significant effects on RAW264.7 cell growth, whereas $C_{60}(OH)_{24}$ alone or CB and $C_{60}(OH)_{24}$ together with oxidized low-density lipoprotein (Ox-LDL) (100 μg/ml) induced cytotoxic morphological changes, such as Ox-LDL uptake-induced foam cell-like formation and decreased cell growth, in a dose-dependent manner. $C_{60}(OH)_{24}$ induced LOX-1 protein expression, pro-matrix metalloprotease-9 protein secretion, and tissue factor mRNA expression in lipid-laden macrophages. Although CB or $C_{60}(OH)_{24}$ alone did not induce platelet aggregation, $C_{60}(OH)_{24}$ facilitated adenosine diphosphate (ADP)-induced platelet aggregation. Furthermore, $C_{60}(OH)_{24}$ acted as a competitive inhibitor of ADP receptor antagonists in ADP-mediated platelet aggregation.

Conclusions The present study confirmed novel effects of nanomaterials in macrophages and platelets. These effects suggest that exposure to nanomaterials might be a risk for atherothrombotic diseases. (*Circ J* 2007; **71:** 437–444)

Key Words: Atherosclerosis; Lipid-laden macrophages; Nanomaterials; Platelet aggregation

The advent of nanomaterials has provided incredible opportunities for biomedical applications such as therapeutic and diagnostic tools, in addition to applications in engineering, electronics and optics.[1–3] Biomedical applications under development include targeted drug delivery systems for the brain and tumor tissues and intravascular nanosensor and nanorobotic devices for imaging and diagnosis. However, the potential adverse effects of nanomaterials on human health remains to be established.[4–6]

Potential exposure pathways for nanomaterials have been proposed in humans.[5,7] Although inhalation might be a major route of exposure, ingestion and dermal exposure are also possible during the nanomaterial manufacture. After inhalation, nanomaterials are deposited in the respiratory tract, and their small size allows cellular uptake and transcytosis into the blood and lymphatic system. Our experiments have shown that both carbon black (CB) and water-soluble fullerene ($C_{60}(OH)_{24}$) exhibit cytotoxicity in human umbilical vein endothelial cells (HUVEC), such as decreased cell density and cell growth. Furthermore, CB and $C_{60}(OH)_{24}$ upregulated the expression of inflammation-related genes and ubiquitin-proteasome-related genes in HUVEC. These results suggest that exposure to CB and/or $C_{60}(OH)_{24}$ might be a risk for atherothrombotic diseases.[8,9]

(Received June 13, 2006; revised manuscript received December 6, 2006; accepted December 19, 2006)

Department of Epidemiology, Research Institute, National Cardiovascular Center, Suita, Japan

Mailing address: Yasuharu Niwa, PhD, Department of Epidemiology, Research Institute, National Cardiovascular Center, Suita 565-8565, Japan. E-mail: yniwa@ri.ncvc.go.jp

In addition to endothelium, macrophages and platelets are important players for atherogenesis. Macrophages under the endothelium may take up denatured-low-density lipoprotein (LDL) (oxidized-LDL; Ox-LDL and acetylated-LDL; Ac-LDL) and become foam cells. The lipid-laden macrophages play a key role in inducing plaque rupture by secreting proteases, such as a matrix metalloprotease-9 (MMP-9) that destroys the extracellular matrix. Finally, rupture of advanced atherosclerotic plaques can lead to platelet aggregation, which results in atherothrombotic events.

In the present study, we aimed to clarify the effects of chronic exposure of nanomaterials, such as CB and $C_{60}(OH)_{24}$, on macrophages phenotypes and the aggregating effects of CB and $C_{60}(OH)_{24}$ on platelets.

Methods

Materials

CB (Association of Powder Process Industry and Engineering, Japan) and $C_{60}(OH)_{24}$ (Tokyo Progress Sysytem, Tokyo, Japan) were prepared as described previously.[9] Fluoresbrite carboxylate microspheres (diameter, 6 μm) were obtained from Polysciences Inc (PA, USA).

Cell Culture

Mouse macrophages cell lines (RAW264.7) were obtained from Dainippon Sumitomo Phrma (Osaka, Japan) and were cultured in RPMI1640 with 10% (v/v) fetal bovine serum (Hyclone, Utah, USA). Cells were cultured in RPMI1640 with 2% (v/v) fetal bovine serum plus sonicated CB (0–100 μg/ml) or $C_{60}(OH)_{24}$. Cells were passaged every 3–4 days.

Lactate Dehydrogenase (LDH) Assay

LDH activity was analyzed with a CytoTox 96 non-radioactive cytotoxicity assay kit (Promega, Madison, USA) according to the manufacturer's protocols. RAW264.7 cells at 50–60% confluence were treated with CB or $C_{60}(OH)_{24}$ alone for 24 h, or 13 or 50 days. In addition, cells at 50–60% confluence were treated with CB or $C_{60}(OH)_{24}$ for 50 days or 8 days, respectively, and Ox-LDL was then added (Biomedical Technologies, MA, USA) (0–100 μg/ml) for a further 2 days. LDH activity in the culture medium was measured based on absorbance at 490 nm using a microplate reader (ARVO; PerkinElmer, Japan). Cytotoxicity was expressed relative to basal LDH release in untreated controls. Cells at 50–60% confluence were treated with $C_{60}(OH)_{24}$ for 8 days or 6-μm beads for 3 days, and Ox-LDL or Dil-Ac-LDL (Biomedical Technologies) was then added for 24 h. Cells were examined under a microscope (Zeiss Axiovert 25, Göttingen, Germany).

Proliferation Assay

Cell proliferation assay was carried out using a Cell Counting-8 kit (Dojindo Laboratories, Kumamoto, Japan) according to the manufacturer's protocols. Cells were cultured in 12-well plates, and were treated with Ox-LDL (100 μg/ml) for 5 days to induce foam cell-like formation, after which $C_{60}(OH)_{24}$ (0–100 ng/ml) was added to the cells for a further 2 days. Cell growth was measured based on absorbance at 450 nm as detected by the ARVO micro-plate reader.

Treated and untreated cells were fixed with 4% paraformaldehyde for 15 min at room temperature. After washing, cells were stained with filtered Oil Red O solution (60% isopropanol) or Giemsa solution for 0.5 h–2 h at room temperature. After washing, the cells were examined under a microscope (Olympus BX-51, Tokyo, Japan). The Dil-Ac-LDL incorporated macrophages were captured directly from an RGB camera attached to the microscope (Zeiss Axiovert 25, Göttingen, Germany) and displayed on a Adobe photoshop CS2 to quantify fluoro-intensity in macrophages.

Western Blotting of LOX-1 and SR-AI

Samples were obtained from RAW264.7 cells treated with lysis buffer (20 mmol/L Tris-HCl, pH 7.4, with 150 mmol/L NaCl, 1 mmol/L EDTA, 1 mmol/L EGTA, 2.5 mmol/L sodium pyrophosphate, 1 mmol/L β-glycerol phosphate, 1 mmol/L Na_3VO_4, 1 μg/ml leupeptin, 0.1% protease inhibitor cocktail (Nacarai Tesque, Kyoto, Japan), and 1% Triton X-100). Equal amounts of proteins (10 μg/ml) were subjected to reducing sodium dodecylsulfate–polyacrlamide gel (10%) electrophoresis electrophoresis after boiling with 1 mmol/L dithiothreithol and were transferred to nitrocellulose membranes (Pall Corporation, Ann Arbor, MI, USA). After blocking with 5% (w/v) skim-milk in T-TBS (10 mmol/L Tris-HCl, pH 7.5 with 10 mmol/L sodium chloride and 0.1% Tween 20) buffer, the membrane was incubated with primary antibody (R&D biosystems, MN, USA) (LOX-1; 1:100 dilution, scavenger receptor-type AI (SR-AI); 2 μg/ml) at 4°C overnight. After washing, the membrane was incubated with secondary antibody (anti-mouse horseradish peroxidase-conjugated antibody and anti-rat horseradish peroxidase-conjugated antibody, respectively; 1:5,000-10,000 dilution) at room temperature for 1 h. LOX-1, SR-AI and β-actin protein were visualized using the ECL system (Amersham Biosciences, Buckinghamshire, UK).

Pro-MMP-9 Secretion Assay

Culture medium was collected from cells treated with $C_{60}(OH)_{24}$ alone for 10 days or with $C_{60}(OH)_{24}$ for 8 days followed by 2 days of co-treatment with Ox-LDL (100 μg/ml). Pro-MMP-9 in culture medium was analyzed using a mouse pro-MMP-9 sandwich enzyme-linked immunosorbent assay kit (B&D systems, MN, USA) according to the manufacturer's protocols. Pro-MMP-9 in culture medium was detected by absorbance at 450 nm, and concentration was calculated using a standard curve.

Reverse Transcription (RT)-Polymerase Chain Reaction (PCR) for Tissue Factor mRNA Expression

Expression of tissue factor mRNA in cells treated with $C_{60}(OH)_{24}$ alone for 10 days or with $C_{60}(OH)_{24}$ for 8 days followed by 2 days with Ox-LDL (100 μg/ml) and were quantified by RT-PCR. Tissue factor primer sets were as follows: tissue factor; forward 5'-CGGGTGCAGGCATT CCAGAG-3' and reverse 5'-CTCCGTGGGACAGAGAG-GAC-3', glucose-3-phosphate dehydrogenase; forward 5'-ACCACAGTCCATGCCATCA-3' and reverse 5'-TCCAC CACCCTGTTGCTGTA-3'. The PCR products were electrophoresed on 2% agarose gels, and were stained with ethidium bromide, visualized using ultraviolet and recorded. Expression levels of tissue factor were adjusted against glucose-3-phosphate dehydrogenase expression levels.

Platelet Aggregation Assay

Whole blood was collected from the ear artery of male Japanese white rabbits (n=3; body weight, 3–5 kg) into tubes containing 3.8% (w/v) tri-sodium citrate, and were kept at room temperature for 5–10 min. After pre-treatment with or without CB (5 μg/ml) or $C_{60}(OH)_{24}$ (5 μg/ml) at room temperature for 5 min, ticlopydine hydrochloride (0–4 mmol/L) was added to whole blood, which was then left to stand at room temperature for a further 15 min. Adenosine diphosphate (ADP) (0–80 mmol/L) induced aggregation was analyzed using a whole blood filtration pressure aggregometer (WBA analyzer, Yokohama, Japan)[10] Reaction tubes containing 200 μl aliquots of whole blood were placed an incubation chamber at 37°C for 2 min, followed by addition of 22.2 μl of ADP. The pressure rate was standardized using a grading curve of 4 different ADP concentrations (0, 1, 2, 4, 8 mmol/L or 0, 10, 20, 40, 80 mmol/L, respectively) on the x-axis and pressure rate on the y-axis. The concentration of ADP causing an increase in pressure rate was calculated and was applied as the platelet aggregatory threshold index. Experiments were performed at least 3 times.

Statistical Analysis

Data are shown as means ± SD. Statistical evaluation was performed by ANOVA. Values of $p<0.05$ were considered statistically significant.

Results

Effects of CB on RAW264.7

The effects of chronic exposure to CB were examined by treating RAW264.7 cells with CB (0–100 μg/ml) for 24 h, 13 days and 50 days. We observed marked CB (100 μg/ml) uptake in RAW264.7 cells at days 13 and 50 (Figs 1B, d and C, d). However, cytotoxic morphological changes, such as cytosolic phagosome formation, cell disorientation and decreased cell density, were not observed (Figs 1A, B and C, a–d). No significant cytotoxic injury (based on LDH

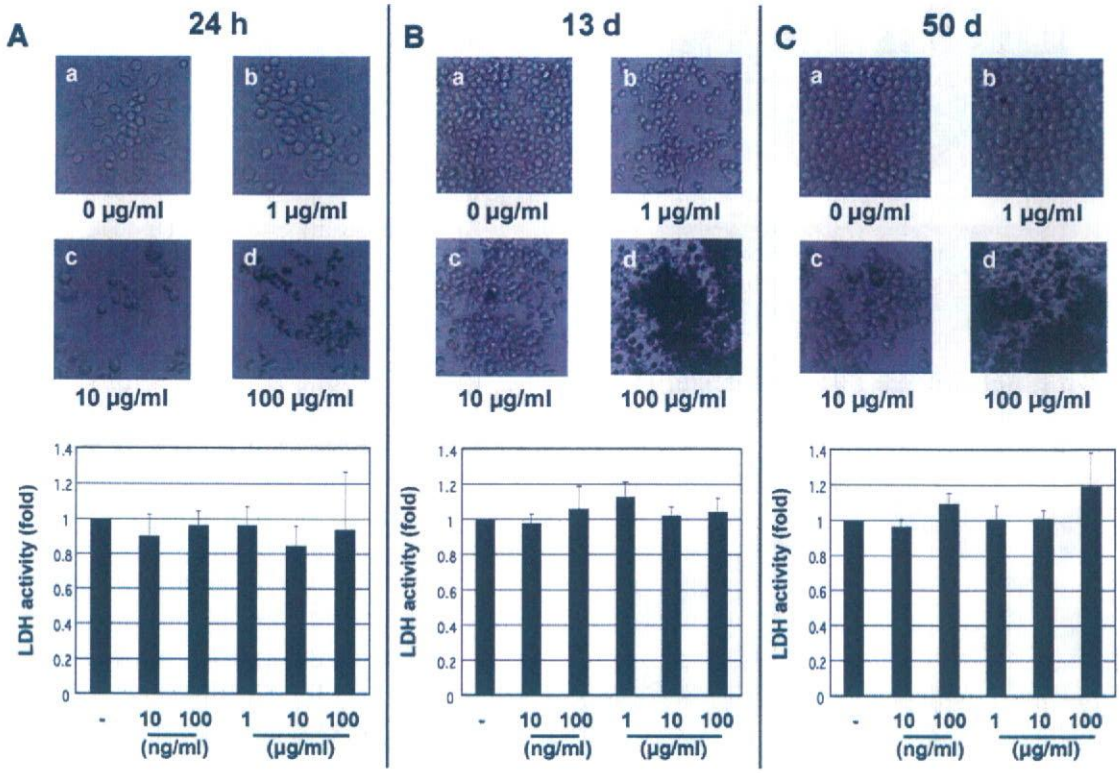

Fig 1. Representative photomicrographs of RAW264.7 cells treated with carbon black (CB). (A) RAW264.7 cells were treated with CB (a, 0 μg/ml; b, 1 μg/ml; c, 10 μg/ml; d, 100 μg/ml) for 24 h, (B) 13 days or (C) 50 days, upper panel (×200 magnification). CB did not induce cytotoxic injury in RAW264.7 cells. RAW264.7 cells were cultured with CB (0, 10 ng/ml, 100 ng/ml, 1 μg/ml, 10 μg/ml or 100 μg/ml) for (A) 24 h, (B) 13 days or (C) 50 days. Culture medium was then collected. Lactate dehydrogenase (LDH) released into supernatant was measured relative to basal LDH release in controls (control ratio=1.0) (n=4), lower panel.

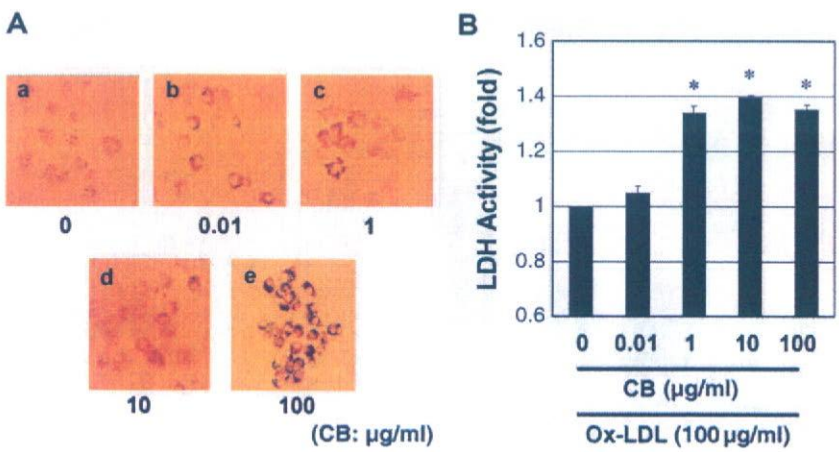

Fig 2. Oxidized low-density lipoprotein (Ox-LDL)-induced cytotoxic injury in carbon black (CB)-treated RAW264.7 cells. (A) After RAW264.7 cells were cultured with CB (a, 0 ng/ml; b, 10 ng/ml; c, 1 μg/ml; d, 10 μg/ml; e, 100 μg/ml) for 48 days, and were then co-treated with Ox-LDL (100 μg/ml) for a further 48 h. Cells were fixed with 4% paraformaldehyde neutralized buffered solution, and were then stained with Oil Red O (a–d). (B) RAW264.7 cells were cultured with CB (0, 10 ng/ml, 100 ng/ml, 1 μg/ml, 10 μg/ml or 100 μg/ml) for 48 days, and were then co-treated with Ox-LDL (100 μg/ml) for a further 48 h. Culture medium was collected, and lactate dehydrogenase (LDH) was measured relative to basal LDH release in controls (CB and Ox-LDL=0 μg/ml) (control ratio=1.0). *$p<0.05$ vs controls.

activity) was seen in RAW264.7 cells at any time point (24 h, 13 days and 50 days) (Figs 1A–C).

CB Together With Ox-LDL Induces Injury in RAW264.7

To determine the effects of Ox-LDL (100 μg/ml) on chronic exposure to CB (0–100 μg/ml) in RAW264.7 cells, we performed Oil Red O staining. Cells were cultured in CB-containing medium for 48 days and were then treated with Ox-LDL for 2 days. Dose-dependent Oil Red O staining was seen with CB treatment (Fig 2A). LDH activity after Ox-LDL treatment was also dependent on CB concentration (peak LDH activity was observed at 10 μg/ml CB) (Fig 2B). These data suggest that CB itself may not be cytotoxic to RAW264.7 cells, but when cells are co-treated with CB and Ox-LDL, LDH secretion was elevated in a CB dose-dependent manner, and Ox-LDL uptake was also increased.

$C_{60}(OH)_{24}$ Induces Cytotoxic Morphological Changes in RAW264.7

RAW264.7 cells were treated with $C_{60}(OH)_{24}$ for 24 h to 10 days. $C_{60}(OH)_{24}$ (20 ng/ml), which is the predicted natu-

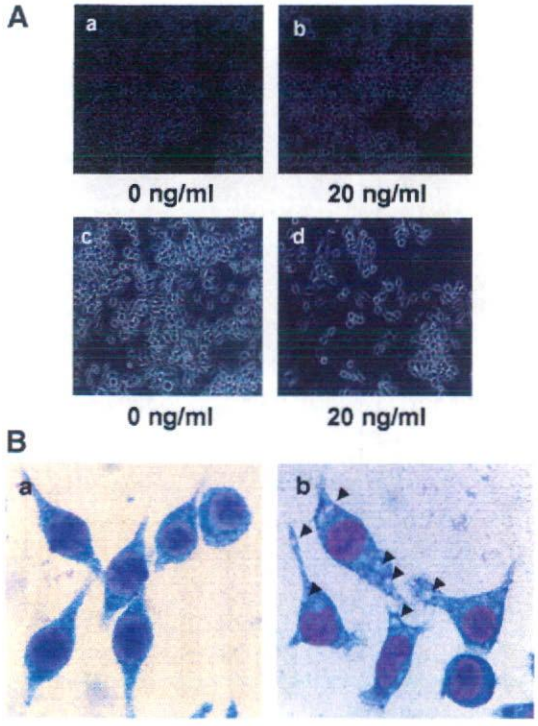

Fig 3. Water-soluble fullerene ($C_{60}(OH)_{24}$) induced phagosome formation in RAW264.7 cells. (A) Cells were treated with $C_{60}(OH)_{24}$ (a, 0 ng/ml; b, 20 ng/ml) for 24 h or 10 days (c, 0 ng/ml; d, 20 ng/ml), and cell morphology was then visualized (×200 magnification). (B) Cells were treated with $C_{60}(OH)_{24}$ (0, 20 ng/ml) for 10 days, and the cells were then fixed with 4% (v/v) paraformaldehyde neutralized buffered solution, and stained with Giemsa. Cells were then examined by microscope (×1,000 magnification). Arrowheads indicate phagosomes.

ral environmental concentration[11] induced cytotoxic morphological changes in RAW264.7, including phagosome-like formation in the cytosol and decreased cell density (Fig 3A). Phagosome formation was confirmed by Giemsa staining (Fig 3B, arrowheads).

$C_{60}(OH)_{24}$ Together With Ox-LDL Induces Injury in RAW264.7

To determine the effects of Ox-LDL (100 μg/ml) on $C_{60}(OH)_{24}$ (0–100 ng/ml)-induced cell injury, we performed Oil Red O staining. Cells were cultured with $C_{60}(OH)_{24}$ for 8 days, and were then co-treated with Ox-LDL for 2 days. Enhanced Oil Red O staining was seen in a dose-dependent manner with $C_{60}(OH)_{24}$ and Ox-LDL co-treatment (Figs 4A, d–f), but Oil Red O staining cells was not seen when treated with $C_{60}(OH)_{24}$ alone (Figs 4A, a–c). Increases in LDH activity were dependent on $C_{60}(OH)_{24}$ concentration (LDH maximum activity was observed at 100 ng/ml $C_{60}(OH)_{24}$) in the presence of Ox-LDL (Fig 4B). RAW264.7 cells were also treated with Ox-LDL (100 μg/ml) for 5 days followed by $C_{60}(OH)_{24}$ (20, 100 ng/ml) for a further 48 h. Cells were stained by Oil Red O in a $C_{60}(OH)_{24}$ dose-dependent manner (Fig 4C). In addition, cell growth was dose-dependenly suppressed by $C_{60}(OH)_{24}$ in the pre-treatment with Ox-LDL (Fig 4D). CB alone had no cytotoxic effects, however, $C_{60}(OH)_{24}$ alone had significant cytotoxicities appeared in macrophages. We focused on the characterization of $C_{60}(OH)_{24}$ cytotoxicities in further experiments.

$C_{60}(OH)_{24}$ Induces LOX-1 Expression in RAW264.7

CB and $C_{60}(OH)_{24}$ induced endocytotic uptake of Ox-LDL in RAW264.7 cells, which were strongly stained with Oil Red O. This indicates that expression of Ox-LDL receptors, such as LOX-1, is elevated in RAW264.7 cells. To identify LOX-1 protein expression in RAW264.7, we performed immunoblotting using whole cell extracts. LOX-1 expression was induced by $C_{60}(OH)_{24}$ in a dose-dependent

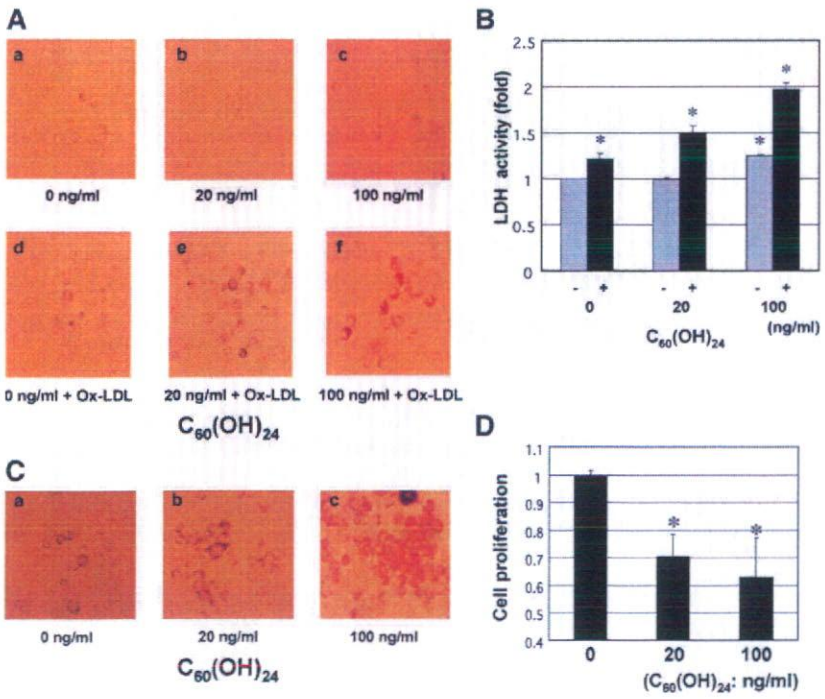

Fig 4. Oxidized low-density lipoprotein (Ox-LDL)-induced cytotoxic injury in water-soluble fullerene ($C_{60}(OH)_{24}$)-treated RAW 264.7 cells. (A) RAW264.7 cells were cultured with $C_{60}(OH)_{24}$ (0 ng/ml, 20 ng/ml, 100 ng/ml) for 8 days and were co-treated with Ox-LDL (100 μg/ml) for a further 48 h. Cells were then fixed with 4% paraformaldehyde neutralized buffered solution and were then stained with Oil Red O (a–f). Cells were visualized by microscopy (×400 magnification). (B) Cells were cultured with $C_{60}(OH)_{24}$ (0, 20 or 100 ng/ml) for 8 days, and were then co-cultured with (+) or without (–) Ox-LDL (100 μg/ml) for a further 48 h. Culture medium was collected and lactate dehydrogenase (LDH) activity was measured. *$p<0.05$ vs controls. (C) RAW264.7 cells were cultured with Ox-LDL (100 μg/ml) for 5 days, and were then co-cultured with $C_{60}(OH)_{24}$ (a, 0 ng/ml; b, 20 ng/ml; c, 100 ng/ml) for a further 48 h. Cells were then fixed and stained with Oil Red O. (D) Cell growth was inhibited by co-treatment with $C_{60}(OH)_{24}$ and Ox-LDL. Cell growth was analyzed using cell counting kit-8. Results are relative to controls (n=4). *$p<0.05$ vs controls.

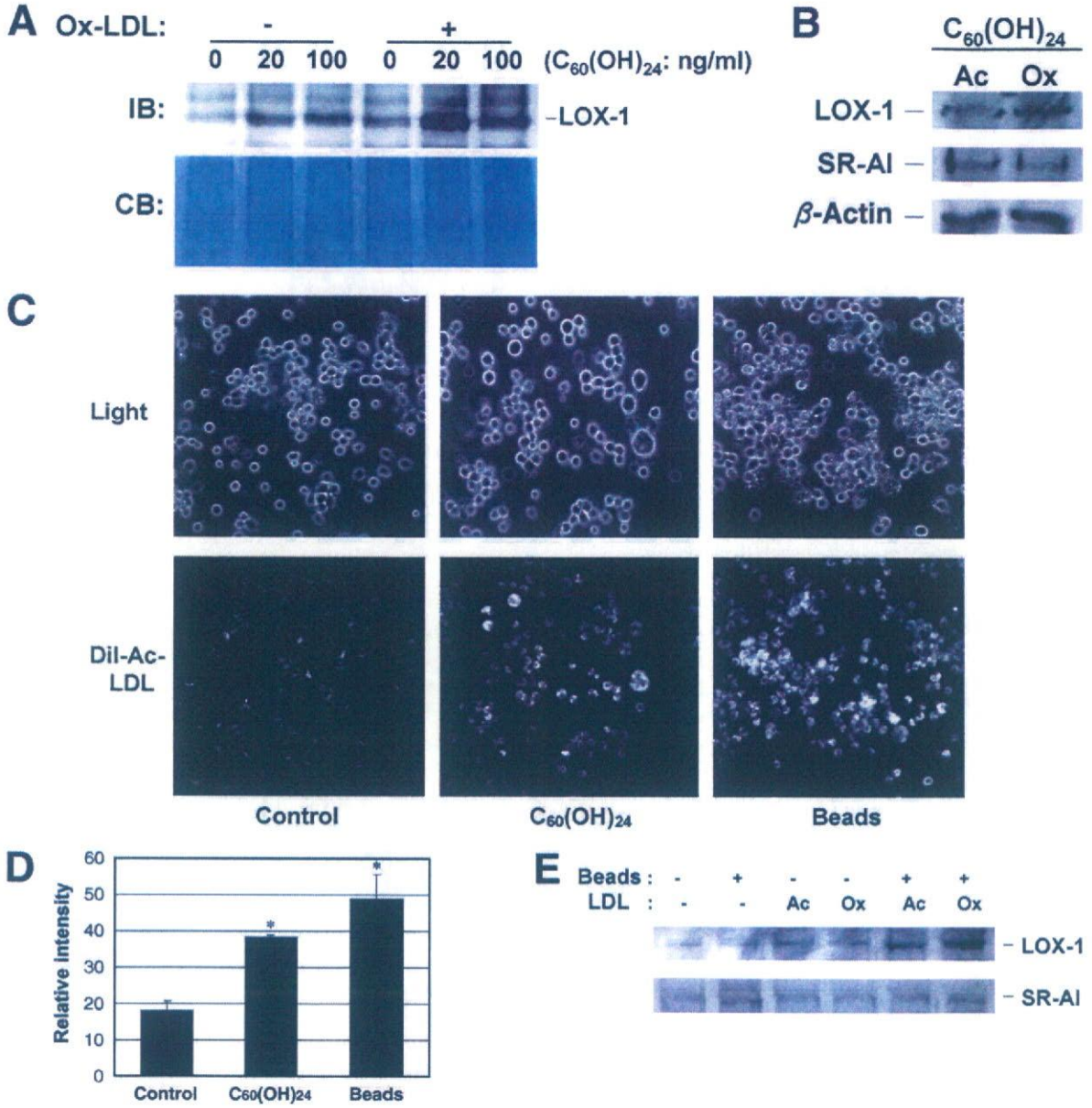

Fig 5. Water-soluble fullerene ($C_{60}(OH)_{24}$) and 6-μm bead-induced LOX-1 expression in RAW264.7 cells. Cells were cultured with $C_{60}(OH)_{24}$ (0, 20 or 100 ng/ml) for 8 days, co-cultured with (+) or without (–) oxidized low-density lipoprotein (Ox-LDL) (100 μg/ml) for a further 48 h and harvested. Whole cell extracts were prepared for sodium dodecylsulfate–polyacrlamide gel electrophoresis (SDS–PAGE). Samples (10 μg/ml) were loaded on reducing SDS–PAGE gels (10%) electrophoresis, and were transferred to membranes for immunoblotting (IB) (LOX-1 1:100, scavenger receptor-type AI (SR-AI): 2 μg/ml). LOX-1 protein or SR-AI protein expression was visualized by enzymatic chemiluminescence (ECL). Equal amounts of protein for Western blotting were confirmed by Coomassie blue staining or β-actin as control (A, B). Dil-acetylated-low-density lipoprotein (Dil-Ac-LDL) incorporation was investigated by pre-treatment with $C_{60}(OH)_{24}$ for 8 days or 6-μm beads for 3 days (beads), or no pre-treatment (control), after which Dil-Ac-LDL (5 μg/ml) was added to RAW264.7 cells. Cells were examined by fluoro-microscopy (×200 magnification) (C). The Dil-Ac-LDL (5 μg/ml) incorporated macrophages were captured directly from RGB camera attached to the microscope and displayed on Adobe photoshop CS2 to quantify of fluoro-intensity in macrophages. $p<0.03$ vs controls (D) Cells were treated with 6-μm beads for 3 days. Ox-LDL or acetylated-LDL was added for 24 h, and cells were harvested. Whole-cell extracts were prepared for SDS–PAGE. Samples (30 μg/ml) were loaded on reducing gels (10%), and were then transferred to membranes for IB (LOX-1 1:100, SR-AI: 2 μg/ml). Protein expression was visualized by ECL (E). CB, carbon black.

manner, and was further stimulated in the presence of Ox-LDL (Fig 5A). In contrast, SR-AI expression was not significantly induced by co-treatment with $C_{60}(OH)_{24}$ and Ox-LDL or Ac-LDL in RAW264.7 cells (Fig 5B). In addition, 6-μm fluoro beads induced endocytotic uptake of Ac-LDL in RAW264.7 cells (Fig 5D). LOX-1 expression was not induced by 6-μm beads, but was stimulated by co-treatment with Ox-LDL or Ac-LDL (Figs 5C,E). LOX-1 protein expression was more strongly stimulated by Ox-LDL than Ac-LDL (Figs 5B,E).

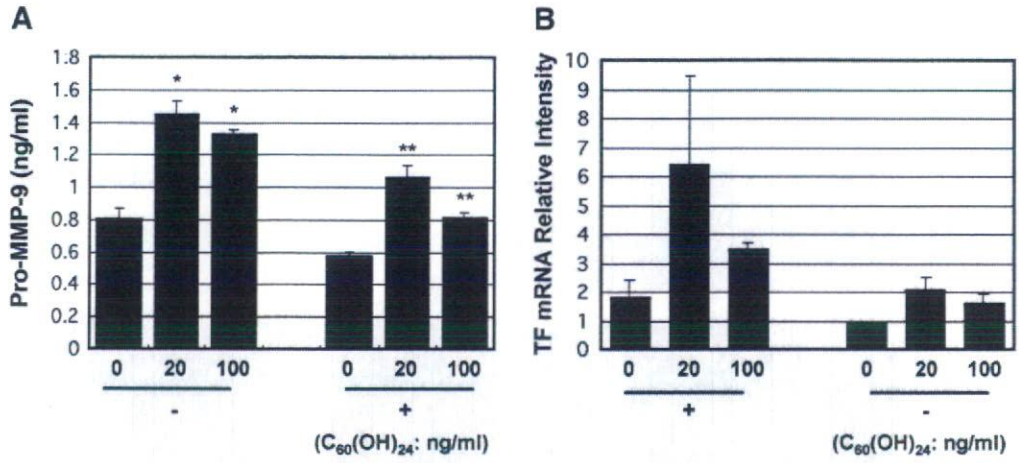

Fig 6. Water-soluble fullerene ($C_{60}(OH)_{24}$)-induced pro-matrix metalloprotease-9 (MMP-9) secretion and tissue factor (TF) mRNA expression. Cells were cultured with $C_{60}(OH)_{24}$ (0, 20 or 100 ng/ml) for 8 days and were then co-cultured with (+) or without (–) oxidized low-density lipoprotein (Ox-LDL) (100 μg/ml) for a further 48 h, after which culture medium was collected for pro-MMP-9 enzyme-linked immunosorbent assay (n=4) (A), and total RNA was extracted from the cells for TF reverse transcription-polymerase chain reaction experiments (n=3) (B). *p<0.02 vs controls (0 ng/ml), **p<0.05 vs controls (0 ng/ml).

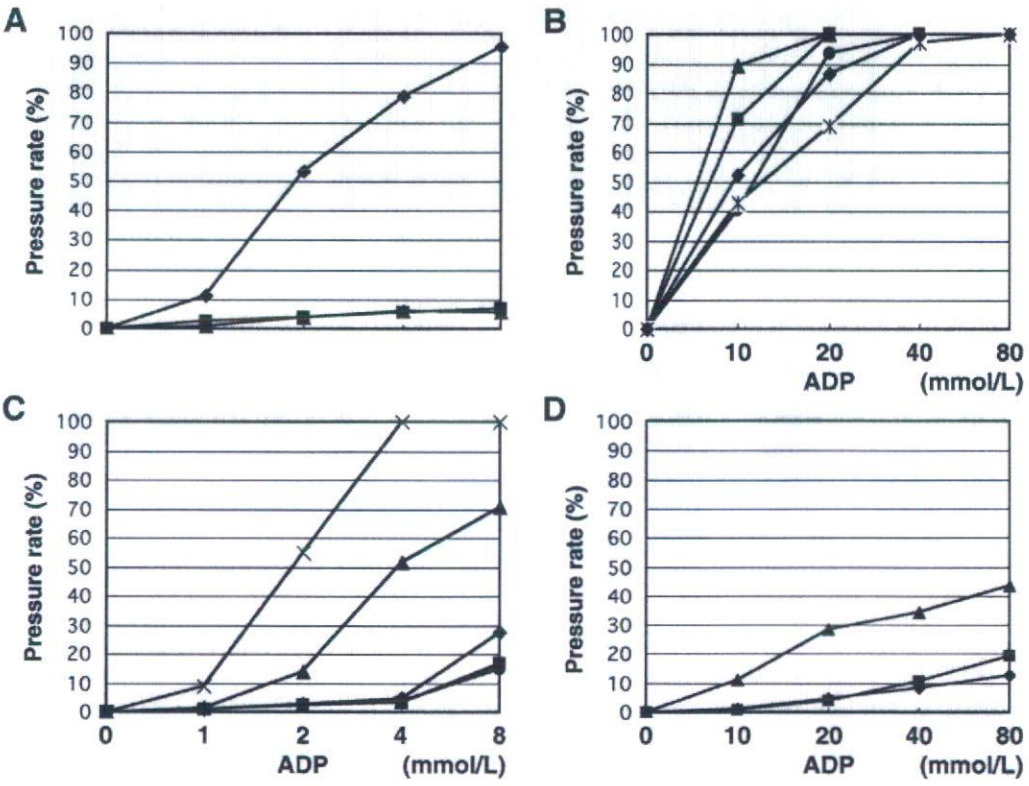

Fig 7. Platelet aggregation, as analyzed by screen filtration pressure method in carbon black (CB) or water-soluble fullerene ($C_{60}(OH)_{24}$)-treated whole blood. (A) Concentration response curve of platelet aggregation to adenosine diphosphate (ADP) (◆; 0, 10, 20, 40, 80 mmol/L), CB (▲; 0, 50, 100, 200 μg/ml) and $C_{60}(OH)_{24}$ (■; 0, 5, 10, 25, 50 μg/ml). (B) High-concentration ADP (●; 0, 10, 20, 40, 80 mmol/L), CB (*; 50 μg/ml, ◆; 100 μg/ml), $C_{60}(OH)_{24}$ (■; 25 μg/ml, ▲; 50 μg/ml), and (C) low-concentration ADP (◆; 0, 1, 2, 4, 8 mmol/L), ADP-induced aggregation was facilitated by $C_{60}(OH)_{24}$ (■; 2.5 μg/ml, ▲; 25 μg/ml, ×; 50 μg/ml) in a dose-dependent manner, but CB (*; 50 μg/ml, ●; 100 μg/ml) had no effect. (D) High-concentration ADP (0, 10, 20, 40, 80 mmol/L), $C_{60}(OH)_{24}$ (■; 2.5 μg/ml, ▲; 10 μg/ml) upregulated platelet aggregation, despite inhibition by ticlopidine hydrochloride (◆; 2 mmol/L).

$C_{60}(OH)_{24}$ Induces Pro-MMP-9 Secretion and Tissue Factor mRNA Expression in RAW264.7

To assess whether pro-MMP-9 may be secreted from in RAW264.7 cells, cells were treated with $C_{60}(OH)_{24}$ (0–100 ng/ml) for 8 days and Ox-LDL (100 μg/ml) was added for 2 further days of culture. Sandwich ELISA against for pro-MMP-9 was then performed. The amounts of pro-MMP-9 secreted into culture medium were significantly increased in the presence of $C_{60}(OH)_{24}$, and under co-treatment conditions with Ox-LDL and $C_{60}(OH)_{24}$, although the amount of secreted pro-MMP-9 was 25% lower under the co-treatment conditions (Fig 6A). Tissue factor mRNA expression was approximately 2-fold higher with $C_{60}(OH)_{24}$, and was approximately 6-fold higher after $C_{60}(OH)_{24}$ stimulation (Fig 6B). These results show that $C_{60}(OH)_{24}$ alone facilitates pro-MMP-9 secretion and tissue factor mRNA expression via an unknown pathway in RAW264.7 cells.

$C_{60}(OH)_{24}$ and CB Effects on Platelet Aggregation

The effects of CB or $C_{60}(OH)_{24}$ on platelet function were examined by evaluating ADP-induced whole blood aggregation using the filtration pressure method. $C_{60}(OH)_{24}$ does not stimulate platelet aggregation in vitro[12] We also found that CB and $C_{60}(OH)_{24}$ alone do not induce platelet aggregation (Fig 7A). However, we hypothesized that CB or $C_{60}(OH)_{24}$ might affect ADP-dependent platelet aggregation. When whole blood was pretreated with $C_{60}(OH)_{24}$, ADP-induced aggregation threshold index values were elevated in a dose-dependent manner (Figs 7B,C). Thus, $C_{60}(OH)_{24}$ facilitates ADP-induced aggregation, and this function was dependent on the ADP receptor (Fig 7D), as collagen- and thrombin-induced platelet aggregation threshold index values did not significantly change when whole blood was pre-treated with CB or $C_{60}(OH)_{24}$ (data not shown). These results show that $C_{60}(OH)_{24}$ specifically facilitates ADP-induced platelet aggregation.

Discussion

Epidemiologic and animal studies have suggested that exposure to nanoparticles plays a role in cardiovascular diseases such as atherosclerosis and myocardial infarction[13–20] For example, traffic-derived nanoparticles are suspected to be a risk for cardiovascular diseases[21]

Our studies have recently shown that CB and $C_{60}(OH)_{24}$ exert cytotoxic effects on HUVEC, presumably via phagocytotic cell death dependent on further ubiquitination of cytosolic proteins[9] Endothelial cell injury, inflammation, and impairment of membrane integrity are closely related to the initiation of atherosclerosis and ischemic heart disease[22,23] Nanomaterial cytotoxicity in cells varies with chemical characteristics and surface properties of the molecule, including hydrophobicity, hydrophilicity and surface area per molecule[4,18] The purpose of the current study was to clarify the effects of chronic exposure to low-dose nanomaterials, such as CB or $C_{60}(OH)_{24}$, particularly with regard to the cardiovascular system in vitro and in vivo. The present study indicates that CB alone has no significant cytotoxic actions in macrophages; however, cytotoxicity was markedly enhanced by co-treatment with Ox-LDL. In contrast, $C_{60}(OH)_{24}$ alone has significant cytotoxic actions and cytotoxicity was markedly enhanced by co-treatment with Ox-LDL (Figs 2B,4B).

We analyzed the phagocytotic functions of RAW264.7 cells toward Ox-LDL or Ac-LDL after pre-treatment with 6-μm fluoro beads or 20 ng/ml $C_{60}(OH)_{24}$ in cells. Treatment with 6-μm fluoro beads stimulated Ac-LDL incorporation to a greater degree than pre-treatment with $C_{60}(OH)_{24}$ in RAW264.7 cells (Fig 5D). We proposed that microparticles, as well as nanoparticles, are able to stimulate phagocytotic system: however, microparticles more strongly stimulated the phagocytotic function of RAW264.7 cells. Further stimulated phagocytotic function caused cell death in RAW264.7 cells treated with 6-μm fluoro beads for 4 days (data not shown). Interestingly, $C_{60}(OH)_{24}$ alone might induce LOX-1 protein expression; $C_{60}(OH)_{24}$ activated stress-related kinases, such as p38 MAPK, thus contribute to phagosome maturation in macrophages[24,25] and leading to activation of nuclear factor (NF)-κB, which is a major transcriptional factor for LOX-1[26] LOX-1 gene expression is dynamically modulated by tumor necrosis factor-α, transform growth factor-β, angiotensin II, endothelin-1 and peroxisome proliferator-activated receptor-a via NF-κB activation[27–29] and stimulate cell injury or suppress cell growth. Nanomaterials might affect the activity of Ox-LDL receptors, such as CD36, SR-A and LOX-1, on the macrophage plasma membrane, thus triggering the process of phagocytosis and Ox-LDL uptake. We also found that $C_{60}(OH)_{24}$ induced secretion of pro-MMP-9. Macrophage-mediated proteolysis participates in the rupture of atherosclerotic plaques and MMP-9 might be involved in this process. Recent studies have indicated that the proteolytic activity of MMP-9 is sufficient to induce the rupture of advanced atherosclerotic lesions in apoE-/- mice[30,31] These results suggest that nanomaterials might contribute to the rupture of advanced atherosclerosis by stimulating MMP-9 secretion from macrophage-derived foam cells.

CB and $C_{60}(OH)_{24}$ did not directly cause activation and aggregation of platelets in vitro. This observation was also reported by Radomski et al in experiments on nanomaterials and platelet aggregation[12] Although $C_{60}(OH)_{24}$ alone did not activate platelet aggregation, when platelets were pre-treated with $C_{60}(OH)_{24}$, ADP-induced aggregation was 10–20% higher and this increase was $C_{60}(OH)_{24}$ dose-dependent (Figs 7B,C). Furthermore, ADP-induced platelet aggregation was inhibited by more than 80% by ticlopidine hydrochloride (2–4 mmol/L), an ADP receptor (P2Y12) antagonist[32] but after platelets were pre-treated with $C_{60}(OH)_{24}$, inhibition by ticlopidine hydrochloride (2 mmol/L) was suppressed. This indicates that $C_{60}(OH)_{24}$ increases the affinity of ADP for its receptor, possibly via a $C_{60}(OH)_{24}$-dependent conformational change or via $C_{60}(OH)_{24}$-mediated inhibition of ticlopidine hydrochloride binding to P2Y12. Interestingly, $C_{60}(OH)_{24}$ did not affect collagen- or thrombin-induced platelet aggregation (data not shown). $C_{60}(OH)_{24}$ also failed to affect acetylsalicylic acid (aspirin)-mediated inhibition of collagen-induced aggregation, and RGDS peptide-mediated inhibition of thrombin-induced aggregation (data not shown). These results suggest that $C_{60}(OH)_{24}$ specifically stimulates ADP-induced platelet aggregation via an ADP receptor such as P2Y12, and that $C_{60}(OH)_{24}$ might contribute to thrombosis.

We used the ng/ml or μg/ml order concentration of CB and $C_{60}(OH)_{24}$ in experiments of macrophages. This concentration is similar to the maximal concentration of particulate matter <2.5 μm (PM2.5) in Chongqing, a city in China, ~700 μg/m^3 (daily average), and thus an individual might inhale 10,000 μg of particulate matter in a 24 h period. This is equivalent to approximately 1 μg/ml, considering that the extracellular fluid volume of a 60 kg individual is

12 L. However, the effective concentration of CB and $C_{60}(OH)_{24}$ was much higher than predicted physiological concentration in platelet experiments[12]

Taken together, the present results show that the effects of CB or $C_{60}(OH)_{24}$ on macrophage and platelet function contributes to cardiovascular diseases such as atherosclerosis, thrombosis and myocardial infarction. However, further experiments regarding the influence of nanomaterials on the cardiovascular system in vivo are required.

Acknowledgment

This study was supported by a Health and Labor Sciences Research Grant for Research on Risks of Chemical Substances (H17-chemistry-008 to N.I.) and a Grant-in-Aid for Scientific Research (#18590583 to Y.N.) from the Ministry of Education, Culture, Sports, Science and Technology of Japan.

References

1. Akerman ME, Chan WC, Laakkonen P, Bhatia SN, Ruoslahti E. Nanocrystal targeting in vivo. *Proc Natl Acad Sci USA* 2002; **99:** 12617–12621.
2. Borm PJ, Kreyling W. Toxicological hazards of inhaled nanoparticles–potential implications for drug delivery. *J Nanosci Nanotechnol* 2004; **4:** 521–531.
3. Kreuter J. Nanoparticulate systems for brain delivery of drugs. *Adv Drug Deliv Rev* 2001; **47:** 65–81.
4. Colvin VL. The potential environmental impact of engineered nanomaterials. *Nat Biotechnol* 2003; **21:** 1166–1170.
5. Oberdorster G, Oberdorster E, Oberdorster J. Nanotoxicology: An emerging discipline evolving from studies of ultrafine particles. *Environ Health Perspect* 2005; **113:** 823–839.
6. Jia G, Wang H, Yan L, Wang X, Pei R, Yan T, et al. Cytotoxicity of carbon nanomaterials: Single-wall nanotube, multi-wall nanotube, and fullerene. *Environ Sci Technol* 2005; **39:** 1378–1383.
7. Yamago S, Tokuyama H, Nakamura E, Kikuchi K, Kananishi S, Sueki K, et al. In vivo biological behavior of a water-miscible fullerene: 14C labeling, absorption, distribution, excretion and acute toxicity. *Chem Biol* 1995; **2:** 385–389.
8. Yamawaki H, Iwai N. Cytotoxicity of water-soluble fullerene in vascular endothelial cells. *Am J Physiol Cell Physiol* 2006; **290:** C1495–C1502.
9. Yamawaki H, Iwai N. Mechanisms underlying nano-sized air-pollution-mediated progression of atherosclerosis: Carbon black causes cytotoxic injury/inflammation and inhibits cell growth in vascular endothelial cells. *Circ J* 2006; **70:** 129–140.
10. Ozeki Y, Sudo T, Toga K, Nagamura Y, Ito H, Ogawa T, et al. Characterization of whole blood aggregation with a new type of aggregometer by a screen filtration pressure method. *Thromb Res* 2001; **101:** 65–72.
11. Monteil-Rivera F, Beaulieu C, Deschamps S, Paquet L, Hawari J. Determination of explosives in environmental water samples by solid-phase microextraction-liquid chromatography. *J Chromatogr A* 2004; **1048:** 213–221.
12. Radomski A, Jurasz P, Alonso-Escolano D, Drews M, Morandi M, Malinski T, et al. Nanoparticle-induced platelet aggregation and vascular thrombosis. *Br J Pharmacol* 2005; **146:** 882–893.
13. Brook RD, Franklin B, Cascio W, Hong Y, Howard G, Lipsett M, et al; Expert Panel on Population and Prevention Science of the American Heart Association. Air pollution and cardiovascular disease: A statement for healthcare professionals from the Expert Panel on Population and Prevention Science of the American Heart Association. *Circulation* 2004; **109:** 2655–2671.
14. Nemmar A, Hoet PH, Vanquickenborne B, Dinsdale D, Thomeer M, Hoylaerts MF, et al. Passage of inhaled particles into the blood circulation in humans. *Circulation* 2002; **105:** 411–414.
15. Nemmar A, Hoet PH, Dinsdale D, Vermylen J, Hoylaerts MF, Nemery B, et al. Diesel exhaust particles in lung acutely enhance experimental peripheral thrombosis. *Circulation* 2003; **107:** 1202–1208.
16. Peters A, Dockery DW, Muller JE, Mittleman MA. Increased particulate air pollution and the triggering of myocardial infarction. *Circulation* 2001; **103:** 2810–2815.
17. Bonetti PO, Lerman LO, Lerman A. Endothelial dysfunction: A marker of atherosclerotic risk. *Arterioscler Thromb Vasc Biol* 2003; **23:** 168–175.
18. Bosi S, Feruglio L, Da Ros T, Spalluto G, Gregoretti B, Terdoslavich M, et al. Hemolytic effects of water-soluble fullerene derivatives. *J Med Chem* 2004; **47:** 6711–6715.
19. Katsouyanni K, Touloumi G, Samouli E, Gryparis A, Le Tertre A, Monopolis Y, et al. Confounding and effect modification in the short-term effects of ambient particles on total mortality: Results from 29 European cities within the APHEA2 project. *Epidemiology* 2001; **12:** 521–531.
20. Dockery DW, Pope CA 3rd, Xu X, Spengler JD, Ware JH, Fay ME, et al. An association between air pollution and mortality in six U.S. cities. *N Engl J Med* 1993; **329:** 1753–1759.
21. Nemmar A, Hoet PH, Vermylen J, Nemery B, Hoylaerts MF. Pharmacological stabilization of mast cells abrogates late thrombotic events induced by diesel exhaust particles in hamsters. *Circulation* 2004; **110:** 1670–1677.
22. Libby P. Inflammation in atherosclerosis. *Nature* 2002; **420:** 868–874.
23. Ross R. Atherosclerosis--an inflammatory disease. *N Engl J Med* 1999; **340:** 115–126.
24. Manna SK, Sarkar S, Barr J, Wise K, Barrera EV, Jejelowo O, et al. Single-walled carbon nanotube induces oxidative stress and activates nuclear transcription factor-kappaB in human keratinocytes. *Nano Lett* 2005; **5:** 1676–1684.
25. Fratti RA, Chua J, Deretic V. Induction of p38 mitogen-activated protein kinase reduces early endosome autoantigen 1 (EEA1) recruitment to phagosomal membranes. *J Biol Chem* 2003; **278:** 46961–46967.
26. Sawamura T, Kume N, Aoyama T, Moriwaki H, Hoshikawa H, Aiba Y, et al. An endothelial receptor for oxidized low-density lipoprotein. *Nature* 1997; **386:** 73–77.
27. Chen M, Masaki T, Sawamura T. LOX-1, the receptor for oxidized low-density lipoprotein identified from endothelial cells: Implications in endothelial dysfunction and atherosclerosis. *Pharmacol Ther* 2002; **95:** 89–100.
28. Moriwaki H, Kume N, Kataoka H, Murase T, Nishi E, Sawamura T, et al. Expression of lectin-like oxidized low density lipoprotein receptor-1 in human and murine macrophages: Upregulated expression by TNF-alpha. *FEBS Lett* 1998; **440:** 29–32.
29. Kume N, Morikawa H, Kataoka H, Minami M, Murase T, Sawamura T, et al. Inducible expression of LOX-1, a novel receptor for oxidized LDL, in macrophages and vascular smooth muscle cells. *Ann N Y Acad Sci* 2000; **902:** 323–327.
30. Luttun A, Lutgens E, Manderveld A, Maris K, Collen D, Carmeliet P, et al. Loss of matrix metalloproteinase-9 or matrix metalloproteinase-12 protects apolipoprotein E-deficient mice against atherosclerotic media destruction but differentially affects plaque growth. *Circulation* 2004; **109:** 1408–1414.
31. Gough PJ, Gomez IG, Wille PT, Raines EW. Macrophage expression of active MMP-9 induces acute plaque disruption in apoE-deficient mice. *J Clin Invest* 2006; **116:** 59–69.
32. Hollopeter G, Jantzen HM, Vincent D, Li G, England L, Ramakrishan V, et al. Identification of the platelet ADP receptor targeted by antithrombotic drugs. *Nature* 2001; **409:** 202–207.

Circ J 2007; **71:** 1157–1161

Nano-Sized Carbon Black Exposure Exacerbates Atherosclerosis in LDL-Receptor Knockout Mice

Yasuharu Niwa, PhD; Yumiko Hiura, PhD; Toshinori Murayama, MD*; Masayuki Yokode, MD*; Naoharu Iwai, MD

Background Associations between exposure to particulate matter and susceptibility to cardiovascular events have been reported. Although the underlying mechanisms are not fully understood, this association seems to be particularly exaggerated in the presence of atherothrombotic risk factors. The present study was undertaken in low-density lipoprotein receptor knockout (LDLR/KO) mice to test the hypothesis that long-term exposure to a high dose of nano-sized carbon black (CB) exacerbates atherosclerotic lesions.

Methods and Results LDLR/KO mice were subjected to a 10-week intratracheal dispersion of CB (1 mg/week) or air under a 0% or 0.51% cholesterol (Chol) diet. Development of aortic lipid-rich lesions was detected in mice under a 0.51% Chol diet with or without CB dispersion, but not in mice fed a 0% Chol diet with or without CB. Quantification of the area stained with oil red O revealed the highest percentage in CB-treated mice on a 0.51% Chol diet among the 4 groups. One-way ANOVA indicated CB-treated mice with 0.51% Chol diet had a significantly higher percentage of positive staining than vehicle-treated mice with 0.51% Chol diet ($p<0.05$).

Conclusions In LDLR-deficient mice under a high Chol diet, exposure to CB resulted in acceleration of development of atherosclerosis. (*Circ J* 2007; **71:** 1157–1161)

Key Words: Atherosclerosis; Epidemiology; Risk factors

Exposure to particulate matter has been recognized as a risk factor for atherothrombotic diseases![1–3] We have previously shown that both carbon black (CB) and water-soluble fullerene ($C_{60}(OH)_{24}$) induce cytotoxic injury, inhibit cell growth and upregulate pro-inflammatory genes such as *ICAM-1*, *E-selectin* and *CCL2* in human umbilical vein endothelial cells (HUVEC), suggesting a possible atherothrombogenic role of nano-sized particulate matter in the development of air-pollution-mediated cardiovascular disease[4,5] Interestingly, in cultured macrophage cells, cytotoxicity of either CB or $C_{60}(OH)_{24}$ was markedly enhanced by co-treatment with oxidized-low-density lipoprotein (LDL), leading to the development of lipid-laden macrophages and secretion of pro-matrix metalloproteinase 9 (pro-MMP9)[6] Therefore, it can be speculated that CB may exacerbate atherosclerosis in the presence of risk factors for cardiovascular disease. In the present study, we tested the hypothesis that exposure to CB may exacerbate atherosclerotic lesions in a model using LDL receptor (LDLR) knockout (LDLR/KO) mice fed a high cholesterol (Chol) diet.

Methods

Animal Model

Male LDLR/KO mice were obtained from the Jackson Laboratory (Bar Harbor, ME, USA). Mice homogeneous for LDLR-null allele were subsequently generated and kept in a temperature-controlled facility on a 12-h light–dark cycle with free access to normal chow and water. At 6 weeks of age, the mice were randomly divided into 4 groups (5 per group). Two groups of mice were subjected to a 10-week endotracheal dispersion of autoclaved CB (1 mg per animal/week) and given isoenergy diets containing 0% or 0.51% Chol. Another 2 groups of mice underwent intratracheal dispersion of air only under isonergy diets with 0% or 0.51% Chol. Intratracheal dispersion of CB and air was performed once a week for 10 weeks under light ether anesthesia using the DP-4 dry powder insufflator (Penn-Century Inc, Philadelphia, PA, USA). CB (The Association of Powder Process Industry and Engineering, Japan) was autoclaved before administration. The distribution of particle size (nm) is presented in Fig 1. At the end of the experiment, the mice were anesthetized by pentobarbital, and then the blood was collected directly from the abdominal aorta. The blood samples were stored at –80°C until analysis.

The acute effect of CB dispersion on circulating levels of C-reactive protein (CRP) was investigated in a separate group of male LDLR/KO mice aged 10–14 weeks. Mice were first fed with a 0.51% Chol diet for 3 days and were subjected to single administration of CB (1 mg per animal) or air using the identical protocol as described above (5 mice each in CB-treated and air-treated groups). Blood samples were collected 24 h after dispersion with CB or air.

All animal experiments were performed in accordance with the institutional ethical guidelines for experiments with animals.

Histochemical Analysis

The extent of atherosclerosis was assessed in the longitu-

(Received January 24, 2007; revised manuscript received March 28, 2007; accepted April 10, 2007)

*Department of Epidemiology, Research Institute, National Cardiovascular Center, Suita, *Department of Clinical Innovative Medicine, Graduate School of Medicine, Kyoto University, Kyoto, Japan*
Yasuharu Niwa and Yumiko Hiura contributed equally to this work.
Mailing address: Naoharu Iwai, MD, Department of Epidemiology, Research Institute, National Cardiovascular Center, 5-7-1 Fujishirodai, Suita 565-8565, Japan. E-mail: iwai@ri.ncvc.go.jp

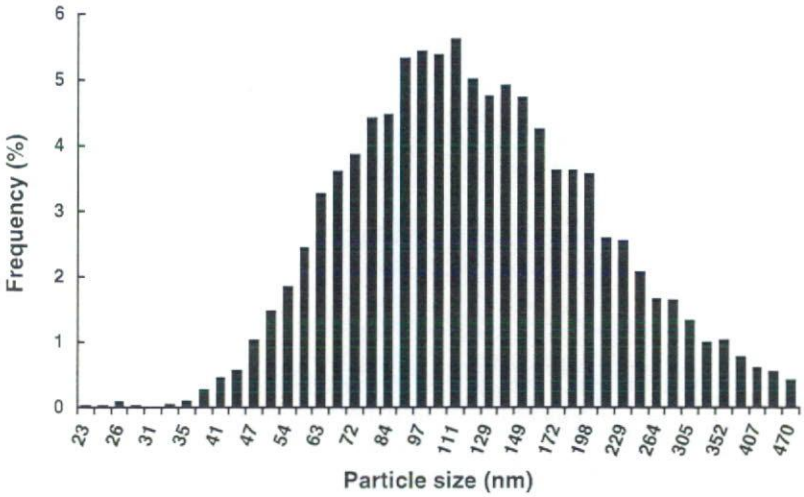

Fig 1. Distribution of carbon black particles (nm). Particle diameter was measured by a Particle Size Analyzer (UPA-EX150, Nikkiso, Japan). Mean size was 120.7 nm (mode = 111.4 nm, geometric SD = 1.68).

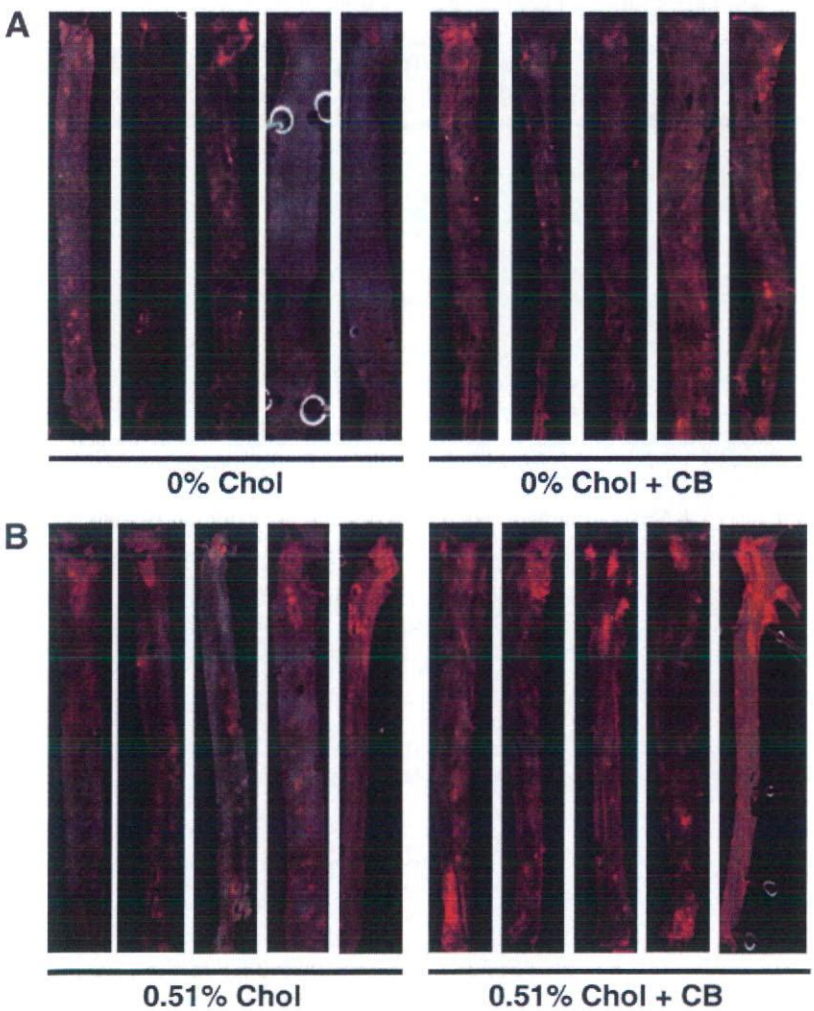

Fig 2. Oil red O staining of the plaque area of aortic tissue samples from low-density lipoprotein receptor knockout (LDLR/KO) mice. The extent of atherosclerosis was assessed in aortas that were opened longitudinally. Representative aortic tissues from LDLR/KO mice on a 0% cholesterol (Chol) diet with or without carbon black (CB) treatment (A) and for those on a 0.51% Chol diet with or without CB treatment (B). Development of lipid-rich aortic lesions is more evident in the mice on the 0.51% Chol diet than in those on the 0% Chol diet.

dinally opened aortas that were stained with oil red O and pinned flat on a dish. The stained aortas were examined under a stereomicroscope (Olympus, model SZX12, Tokyo, Japan) connected to a RGD camera (Olympus, model DP-12). Captured images were analyzed with Adobe Photoshop CS2 to quantify the total surface area of the aorta and the positively stained area, using a square grid as a guide. The positively stained lesion looked brighter in the images than the area not stained with oil red O (Figs 2A,B). The percentage of the stained area was determined by the number of the

Table 1 Characteristics of the 4 Study Groups

	0% Chol	0% Chol+CB	0.51% Chol	0.51% Chol+CB
Baseline body weight (g)	22.7±1.0	21.8±1.0	23.4±1.0	25.0±1.0
Body weight (g)	36.2±5.3	28.1±3.9	48.1±2.9	44.2±2.9
Lung (g)	0.156±0.019	0.142±0.013	0.197±0.035	0.174±0.018
Heart (g)	0.190±0.056	0.144±0.018	0.167±0.025	0.164±0.024
Liver (g)	1.70±0.128	1.32±0.225	2.69±0.514	2.32±0.333
Spleen (g)	0.072±0.008	0.066±0.011	0.090±0.010	0.114±0.033
Kidney, left (g)	0.192±0.034	0.184±0.045	0.210±0.010	0.234±0.052
Kidney, right (g)	0.190±0.023	0.184±0.033	0.210±0.010	0.194±0.005

Organ weights of low-density lipoprotein receptor knockout mice on 0% or 0.51% cholesterol (Chol) diet measured at the end of the 10-week treatment with carbon black (CB) or vehicle are indicated. Body weight was determined at baseline and at the end of experiment (n=5 per group). Data are mean±SD.

grid stained with oil red O (X) divided by the total number (Y) of the grid in the whole vessel area (X/Y×100=Z%). The mean percentage of positively stained area was calculated for each animal.

Electron Microscopic Analysis

Mice tissue samples (aorta, liver, kidney and spleen) were fixed in 0.1 mol/L sodium cacodylate buffer (pH7.4) containing 2.0% glutaraldehyde for 1 h at 4°C, followed by overnight post-fixation with 1.0% osmium tetroxide in 0.1 mol/L sodium cacodylate buffer (pH7.4) at 4°C. After dehydration in an ethanol gradient (50–100%, each for 10 min), samples were embedded in EPON812 at 60°C for 2 days. Ultrathin sections (80 nm) were stained with uranyl acetate and lead citrate. The sections were examined with an electron microscope (JEOL JEM2000X) at 100 kV.

Biochemical Analysis

Total Chol and triglyceride levels were determined by assay kits according to the manufacturer's instructions (Wako, Japan). Concentrations of CRP were measured by ELISA according to the manufacturer's protocol (Life Diagnostics, West Chester, PA, USA).

Statistical Analysis

Results are expressed as mean±SD. Differences in percent area positively stained with oil red O among the 4 groups (0% Chol, 0% Chol+CB, 0.51% Chol and 0.51% Chol+CB) were examined using 1-way ANOVA followed by Tukey-Kramer's HSD test. Comparisons of CRP levels between CB-treated and air-treated groups fed with 0.51% Chol were made by 2-tailed Student's t-test. Statistical analysis was performed using the JMP statistical package 4.0 (SAS Institute, Cary, NC, USA).

Results

The LDLR/KO mice underwent intratracheal dispersion of CB (1 mg per animal) once a week for a total of 10 weeks. Although no difference in body weight between the 4 groups was observed at baseline, and all mice experienced an increase in body weight with advancing age, the mice treated with CB tended to be smaller than those treated with vehicle (Table 1). No significant differences were observed in Chol and triglyceride levels among the 4 groups (data not shown).

Development of aortic lipid-rich lesions occurred in mice under a 0.51% Chol diet with or without CB infusion, but not in the mice fed a 0% Chol diet with or without CB (Figs 2A,B). Quantification of the area stained with oil red O revealed the highest percentage in CB-treated mice on a 0.51% Chol diet among the 4 groups (Fig 3). One-way ANOVA indicated that there were significant differences among the 4 groups ($p<0.0001$). Subsequent comparison revealed CB-treated mice under the 0.51% Chol diet had a significantly higher percentage of positive staining than vehicle-treated mice with the same diet ($p<0.05$, Fig 3).

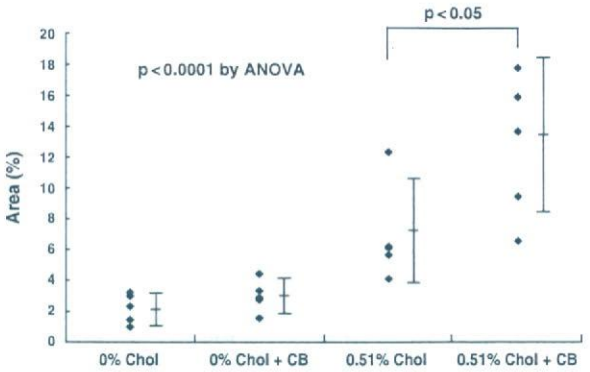

Fig 3. Comparison of the percent area positively stained with oil red O among the groups. Percentage of stained area was quantified by dividing the positively stained area by the total surface area. Each point represents 1 animal. Horizontal bars indicate means (Middle) and SD. Group differences were observed by 1-way ANOVA ($p<0.0001$), with carbon black (CB)-treated mice fed a 0.51% cholesterol (Chol) chow having the highest percentage of positive staining among the 4 groups. Within the group of mice fed a 0.51% Chol diet, mice undergoing intratracheal dispersion of CB had a greater percent area stained with oil red O than the vehicle-treated mice ($p<0.05$).

The effect of a single CB dispersion on circulating levels of CRP was examined in the separate group of mice. Circulating levels of CRP measured 24 h after the single dispersion of CB or air were significantly higher in mice exposed to CB than in mice treated with air (Fig 4, $p=0.0005$), indicating an acute inflammatory response.

Although the presence of CB in pulmonary macrophage-like cells in CB-treated mice under a 0.51% Chol diet was confirmed, CB was not detected by electron microscopic examination of the aortas, livers, kidneys and spleens (data not shown).

Discussion

Our study demonstrates that intratracheal dispersion of CB can induce the development of atherosclerosis in LDLR/KO mice fed a diet with 0.51% Chol. It has previously been shown that 6-month exposure to low concen-

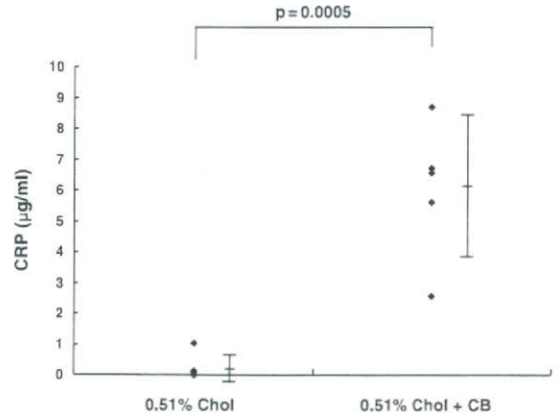

Fig 4. Acute inflammatory response to carbon black (CB) exposure. Circulating levels of C-reactive protein (CRP) were determined 24 h after a single dispersion of CB or air. Distribution of CRP levels in each group (n=5) is shown, with each point representing 1 animal. Horizontal bars indicate means (Middle) and SD. CRP levels were significantly higher in mice exposed to CB than in mice treated with air. Both groups were fed a diet containing 0.51% cholesterol (Chol).

trations of ambient particles of less than 2.5 μm induced acceleration of atherosclerosis in apolipoprotein E-deficient mice under a high-fat diet.[7] Similarly, exposure of particulate matter (<10 μm) for 4 weeks by intrapharyngeal instillation exacerbated the atherosclerotic lesions in the coronary arteries and aortas of rabbits susceptible to the development of atherosclerosis.[8] Our results are in accordance with these findings, despite differences in dosages, length of the experimental period, particle size, animal model and the method of exposure.

Although the exact mechanisms are not yet determined, a study by Nemmar et al has demonstrated the rapid translocation of inhaled nano-sized carbon particles into the bloodstream in humans.[9] CB dispersed into trachea might be translocated into bloodstream and then act as an atherothrombogenic agent on vascular tissues. We have previously shown that nano-sized CB has a direct atherogenic influences on cultured endothelial cells, as indicated by cytotoxicity, inhibition of cell growth and upregulation of pro-inflammatory genes such as *ICAM-1*, *E-selectin* and *CCL2*.[4,5] In addition, our recent study has demonstrated that nano-sized CB exacerbated the formation and cytotoxicity of foam cells (macrophages) induced by the treatment with oxidized-LDL.[6]

Although the rapid translocation of inhaled ^{99m}technetium-labeled carbon particles into the bloodstream in humans has been reported,[9] a more recent study conducted using the same dose of technegas (100 MBq) has found most of the inhaled carbon nanoparticles remained in the lungs (approximately 95% at 6 h after inhalation).[10] Similar observations have been reported in animal models[11] and humans.[12,13] We attempted to clarify whether dispersed CB might be translocated into circulating blood and taken up into atherosclerotic plaques. It was evident that dispersed CB had reached the alveolar regions, as evidenced by the existence of macrophage-like cells containing CB (data not shown). However, electron microscopic examination did not reveal the existence of CB in plaque lesions. Although we cannot exclude the possibility that a trace amount of CB might have translocated into the systemic circulation, such a low level of CB appears to be nontoxic. Our in vitro experiments indicated extremely high concentrations of CB were necessary to cause cytotoxicity in endothelial cells[4] and macrophages.[6]

Our observation that CB dispersion induced atherosclerosis in LDLR/KO mice under a 0.51% Chol diet may be partly explained by higher levels of circulating CRP observed in CB-treated than in air-treated mice in response to acute exposure of CB. A local inflammatory response in the lung as a result of accumulation of inhaled particles may lead to endothelial dysfunction and atherothrombogenesis. As originally proposed by Seaton et al,[14,15] it has been hypothesized that ultrafine particles are able to induce oxidative stress and inflammation in the lung in susceptible populations, exerting detrimental effects on the cardiovascular system through the release of pro-inflammatory mediators and coagulation factors. Results from animal[16] and human[17] studies have shown pulmonary inflammation after inhalation of concentrated ambient air particles, as indicated by the increased neutrophils in the bronchoalveolar lavage fluid. A more recent study examining the acute deleterious effects of intratracheal instillation of 6 different ultrafine carbon particles in mice has demonstrated that those with the smallest diameter (7–12 nm) and the largest surface area (807 m^2/g) among the 6 types of particles yielded the most pronounced inflammatory response in the lung.[18] As expected, a negative association between particle diameter and inflammatory response was reported. It can be speculated that the smaller the particle size is, the deeper it can penetrate into the lungs and reach the alveolar regions, exerting more inflammatory effects than larger particles. Interestingly, it was not the particle size, rather the specific surface area that strongly correlated with the magnitude of pulmonary inflammation in the aforementioned study.[18]

The initial stage of atherogenesis involves endothelial dysfunction and there is increasing evidence to suggest an association between impaired endothelial function and cardiovascular events.[19] Although the detailed mechanisms are far from being understood, there is indirect evidence to support a link between inflammation and endothelial dysfunction. Intriguingly, periodontitis, a highly prevalent inflammatory disease, has been shown to be associated with endothelial dysfunction, and the treatment of this condition has been reported to improve endothelial function.[20]

In conclusion, we investigated the effects of CB dispersion into the trachea on the development of atherosclerosis in LDLR/KO mice under a 0.51% Chol diet, and confirmed that CB exposure resulted in acceleration of development of atherosclerosis. The present study may confirm a possible link between air pollution from automobile exhaust and atherothrombotic disease. Future studies involving ambient exposures at lower concentrations for a longer period will be required to infer the human health risks of fine particulate matter in the environment.

Acknowledgments

The present study was supported by the Health and Labor Science Research Grant: Research on risk of Chemical Substance (H17-Chemistry-008).

References

1. Brook RD, Franklin B, Cascio W, Hong Y, Howard G, Lipsett M, et al. Air pollution and cardiovascular disease: A statement for healthcare professionals from the Expert Panel on Population and Prevention Science of the American Heart Association. *Circulation* 2004;

109: 2655–2671.
2. Dockery DW, Pope CA 3rd, Xu X, Spengler JD, Ware JH, Fay ME, et al. An association between air pollution and mortality in six U.S. cities. *N Engl J Med* 1993; **329:** 1753–1759.
3. Peters A, Dockery DW, Muller JE, Mittleman MA. Increased particulate air pollution and the triggering of myocardial infarction. *Circulation* 2001; **103:** 2810–2815.
4. Yamawaki H, Iwai N. Mechanisms underlying nano-sized air-pollution-mediated progression of atherosclerosis: Carbon black causes cytotoxic injury/inflammation and inhibits cell growth in vascular endothelial cells. *Circ J* 2006; **70:** 129–140.
5. Yamawaki H, Iwai N. Cytotoxicity of water-soluble fullerene in vascular endothelial cells. *Am J Physiol Cell Physiol* 2006; **290:** C1495–C1502.
6. Niwa Y, Iwai N. Nanomaterials induce oxidized low-density lipoprotein cellular uptake in macrophages and platelet aggregation. *Circ J* 2007; **71:** 437–444.
7. Sun Q, Wang A, Jin X, Natanzon A, Duquaine D, Brook RD, et al. Long-term air pollution exposure and acceleration of atherosclerosis and vascular inflammation in an animal model. *JAMA* 2005; **294:** 3003–3010.
8. Suwa T, Hogg JC, Quinlan KB, Ohgami A, Vincent R, van Eeden SF. Particulate air pollution induces progression of atherosclerosis. *J Am Coll Cardiol* 2002; **39:** 935–942.
9. Nemmar A, Hoet PH, Vanquickenborne B, Dinsdale D, Thomeer M, Hoylaerts MF, et al. Passage of inhaled particles into the blood circulation in humans. *Circulation* 2002; **105:** 411–414.
10. Mills NL, Amin N, Robinson SD, Anand A, Davies J, Patel D, et al. Do inhaled carbon nanoparticles translocate directly into the circulation in humans? *Am J Respir Crit Care Med* 2006; **173:** 426–431.
11. Kreyling WG, Semmler M, Erbe F, Mayer P, Takenaka S, Schulz H, et al. Translocation of ultrafine insoluble iridium particles from lung epithelium to extrapulmonary organs is size dependent but very low. *J Toxicol Environ Health A* 2002; **65:** 1513–1530.
12. Wiebert P, Sanchez-Crespo A, Seitz J, Falk R, Philipson K, Kreyling WG, et al. Negligible clearance of ultrafine particles retained in healthy and affected human lungs. *Eur Respir J* 2006; **28:** 286–290.
13. Wiebert P, Sanchez-Crespo A, Falk R, Philipson K, Lundin A, Larsson S, et al. No significant translocation of inhaled 35-nm carbon particles to the circulation in humans. *Inhal Toxicol* 2006; **18:** 741–747.
14. Seaton A, MacNee W, Donaldson K, Godden D. Particulate air pollution and acute health effects. *Lancet* 1995; **345:** 176–178.
15. Donaldson K, Stone V, Seaton A, MacNee W. Ambient particle inhalation and the cardiovascular system: Potential mechanisms. *Environ Health Perspect* 2001; **109**(Suppl 4): 523–527.
16. Clarke RW, Catalano PJ, Koutrakis P, Murthy GG, Sioutas C, Paulauskis J, et al. Urban air particulate inhalation alters pulmonary function and induces pulmonary inflammation in a rodent model of chronic bronchitis. *Inhal Toxicol* 1999; **11:** 637–656.
17. Ghio AJ, Kim C, Devlin RB. Concentrated ambient air particles induce mild pulmonary inflammation in healthy human volunteers. *Am J Respir Crit Care Med* 2000; **162:** 981–988.
18. Stoeger T, Reinhard C, Takenaka S, Schroeppel A, Karg E, Ritter B, et al. Instillation of six different ultrafine carbon particles indicates a surface area threshold dose for acute lung inflammation in mice. *Environ Health Perspect* 2006; **114:** 328–333.
19. Lerman A, Zeiher AM. Endothelial function: Cardiac events. *Circulation* 2005; **111:** 363–368.
20. Tonetti MS, D'Aiuto F, Nibali L, Donald A, Storry C, Parkar M, et al. Treatment of periodontitis and endothelial function. *N Engl J Med* 2007; **356:** 911–920.

Circ J 2008; **72:** 144–149

Inhalation Exposure to Carbon Black Induces Inflammatory Response in Rats

Yasuharu Niwa, PhD*; Yumiko Hiura, PhD*;
Hiromi Sawamura, MS; Naoharu Iwai, MD

Background A link between exposure to fine particulate matter and cardiovascular events has been established. Inhaled nanoparticles are thought to pass through the lungs to reach other tissues via systemic circulation and to induce cell or tissue injuries. It was recently shown that long-term exposure to intra-tracheal dispersion of nano-sized carbon black (CB) exacerbates atherosclerotic lesions in low-density lipoprotein receptor-deficient mice. Because intra-tracheal dispersion of CB may be associated with aggregate formation and may not be an ideal method for CB exposure, whole-body inhalation exposure was used in the present study, the aim of which was to examine whether exposure of rats to nano-sized CB particles by inhalation leads to translocation of these particles into the circulation, exerting direct adverse effects on extrapulmonary tissues.

Methods and Results Sprague-Dawley rats were exposed to a high dose of CB or filtered air for 6 h/day, 5 days a week for a total of 4 weeks. Although the presence of CB was confirmed in pulmonary macrophages, electron microscopic survey did not detect CB in other tissues including liver, spleen and aorta. CB exposure raised blood pressure levels in an exposure-time dependent manner. Levels of circulating inflammatory marker proteins, including monocyte chemoattractant protein-1, interleukin-6, and C-reactive protein, were higher in the CB-treated group than in the controls.

Conclusion Evidence of translocation of inhaled CB was not obtained. It is likely that inhaled nano-sized CB particles form aggregations in the lung and do not exert direct adverse effects on extrapulmonary tissues. Air-pollution-mediated cardiovascular events appear to be induced by the low-grade inflammatory response to the accumulation of aggregated nano-sized particles in the lung. (*Circ J* 2008; **72:** 144–149)

Key Words: Atherosclerosis; Inflammation; Nanoparticles

Exposure to particulate matter air pollution has been reported to be associated with death and hospitalization from cardiovascular causes[1,2] The mechanism by which long-term exposure to fine particulate matter increases the risk of cardiovascular disease remains uncertain. Accelerated atherosclerosis and vulnerability to plaque rupture have been documented in experimental animal models exposed to particulate matter[3,4] and ambient pollution has been correlated with elevated blood pressure (BP)[5–8] and heart rate (HR)[9] in humans. Moreover, the duration of exhaust exposure in highway toll collectors has been shown to be associated with carotid intima–media thickening[10]

We recently showed that a 10-week intra-tracheal dispersion of carbon black (CB) induced atherosclerosis in low-density lipoprotein receptor knock-out (LDLR/KO) mice and the explanation appeared to be the inflammatory responses against deposited CB in the lungs[11] It has been postulated that inhalation of fine particulate matter might cause inflammation in the lung, and that this low-grade and prolonged inflammation might accelerate atherothrombotic diseases[12,13]

On the other hand, a more direct role of nanomaterials has been proposed, based on the study by Nemmar et al that showed rapid translocation of inhaled nano-sized carbon particles into the bloodstream of humans[14] Our in-vitro studies also suggested that nano-sized particulate matter might penetrate alveoli into circulating blood, and might directly damage endothelial cells, activate mononuclear cells, and aggregate platelets to accelerate the formation of atherothrombotic diseases[15–17] In our previous analysis of the effect of CB exposure in LDLR/KO mice[11] CB was not detected in tissues other than the lungs. Thus, it is unlikely that dispersed CB translocates into the circulating blood and directly damages target tissues or cells. However, the method of CB exposure in the previous study was intra-tracheal dispersion, which might not mimic the physiological responses elicited by the common route of exposure in humans. It is possible that CB particles administered by intra-tracheal dispersion may more easily aggregate and deposit in alveolar regions than CB particles dispersed in the respiratory air. With whole-body inhalation exposure to nano-sized CB particles, CB might translocate into circulating blood and reach target tissues. To assess this possibility, we examined whether exposure of rats to nano-sized CB particles by inhalation causes translocation of CB particles into the circulation and increases cardiovascular risk by exerting direct adverse effects on extrapulmonary tissues.

(Received June 24, 2007; revised manuscript received August 26, 2007; accepted September 5, 2007)

Department of Epidemiology, Research Institute, National Cardiovascular Center, Suita, Japan
*These 2 authors contributed equally to this work.
Mailing address: Naoharu Iwai, MD, Department of Epidemiology, Research Institute, National Cardiovascular Center, 5-7-1 Fujishirodai, Suita 565-8565, Japan. E-mail: iwai@ri.ncvc.go.jp

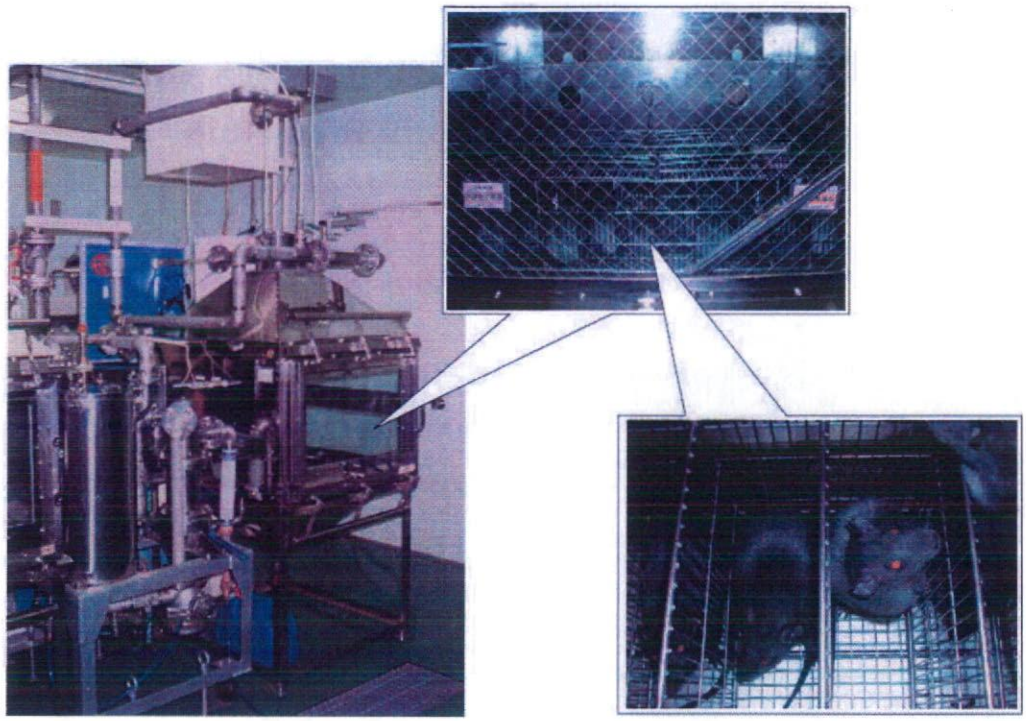

Fig 1. Facility and inhalation chamber used for whole-body inhalation exposure at the facility of the Chemicals Evaluation and Research Institute (CERI, Oita, Japan) using carbon black (CB, Association of Powder Process Industry and Engineering, Kyoto, Japan) generated by a versatile aerosol concentration enrichment system (Dust feeder, Model DF-5, Shibata Kagaku, Tokyo, Japan). Rats were exposed to CB in the inhalation chamber for 6 h/day, 5 days per week for a total of 4 weeks.

Methods

Animal Model

Sprague-Dawley (SD) rats aged 6 weeks (n=50) were obtained from Japan Charles River (Shiga, Japan) and randomly divided into the 2 groups: CB-treated group (n=25) or filtered air-exposed control group (n=25). Rats were housed individually in cages under controlled environment (23°C and 12-h light–dark cycle) with free access to normal chow and tap water. At 1, 7, 14, 28 and 30 days after exposure, 5 rats from each group were killed. They were anesthetized with a high dose of pentobarbital, and then the blood was collected directly from the abdominal aorta, immediately transferred to a tube containing EDTA-2Na or 3.8% sodium citrate and gently mixed. After centrifugation at 1,710 G for 5 min, the supernatant was transferred to a new tube and stored at –80°C until used. The liver, lungs, aorta and spleen were removed and weighed. BP and HR were measured by tail-cuff plethysmography (BP-98A, Softron, Tokyo, Japan) at 1, 14 and 28 days after CB exposure. Mean of 3 measurements was calculated for each rat. Blood samples collected on day 28 or day 30 were used for biochemical analysis. The study protocol was approved by the institutional ethics committee on animal research, and all animal experiments were performed in accordance with the institutional ethical guidelines for experiments with animals.

Exposure to CB

Fig 1 shows the facility and inhalation chamber at the Chemicals Evaluation and Research Institute (CERI, Oita, Japan) where inhalation exposure was carried out. CB (Association of Powder Process Industry and Engineering, Kyoto, Japan) was generated using a versatile aerosol concentration enrichment system (Dust feeder, Model DF-5, Shibata Kagaku, Tokyo, Japan). Rats were exposed to CB in the inhalation chamber at nominal concentrations of 15.6± 3.5 mg/m^3 (1.57±0.4×10^{10} particle number/m^3) for 6 h/day, 5 days per week for a total of 4 weeks. The control rats were exposed to clean, filtered air containing no CB for the same period. The concentrations of CB were monitored twice weekly by measuring the gross weight with a PTFE binder glass filter (TX40HI-20WW, Pall Corporation, NY, USA). Particle diameter of CB was measured by a Particle Size Analyzer (UPA-EX150, Nikkiso, Tokyo, Japan). Mean size (nm)±SD determined at 1, 8, 15, 22 and 29 days after exposure was 118.1±2.4, 119.1±2.7, 122.2±2.0, 122.4±2.5, and 121.9±3.6, respectively. Concentration of CB particles below 100 nm was approximately 3% and 40% of the nominal concentrations of CB particles by weight and by number, respectively.

Biochemical Analysis

Levels of monocyte chemoattractant protein-1 (MCP-1; Pierce Biotechnology Inc, IL, USA), interleukin-6 (IL-6; Pierce Biotechnology Inc), C-reactive protein (CRP; Life diagnostics Inc, PA, USA), and 8-hydroxy-2'-deoxyguanosine (8-OHdG; Japan Institute for the Control of Aging Nikken SEIL Corporation, Shizuoka, Japan) were measured by ELISA according to the manufacturers' protocols. Blood samples collected on day 28 were analyzed for the number of blood cells (red blood cells, white blood cells and platelets) by an automated hematology analyzer (model KX-21NV, Sysmex Corporation, Kobe, Japan).

Table 1 Comparisons of the Hematological and Biochemical Parameters of the CB and Control Groups

	CB (n=5)	Control (n=5)	p value
Red blood cells ($\times 10^4/\mu l$)	727.6±12.7	713.6±38.6	NS
White blood cells ($\times 10^2/\mu l$)	55.8±10.3	67.2±20.8	NS
Platelets ($\times 10^4/\mu l$)	105.1±10.8	98.8±5.9	NS
Creatine kinase (U/L)	531.4±130.9	871.6±412.1	NS
Creatinine (mg/dl)	0.196±0.053	0.236±0.023	NS
AST (IU/L)	109.4±52.5	98.2±38.7	NS
ALT (IU/L)	30.4±7.2	35.6±9.9	NS
Serum albumin (g/dl)	3.7±0.5	3.7±0.3	NS
8-OHdG (ng/ml)	7.0±3.1	4.6±2.4	NS
IL-6 (pg/ml)	34.4±27.0	1.6±2.8	0.05
CRP (μg/ml)	88.4±21.2	28.9±6.0	0.0003
MCP-1 (pg/ml)	2,351.3±250.3	1,105.7±426.8	0.0024

Blood samples collected on day 30 were used for the measurement of creatine kinase, creatinine, AST, ALT and albumin, whereas red blood cells, white blood cells, platelets, 8-OHdG, IL-6, CRP and MCP-1 were determined using blood samples collected on day 28. Differences between the groups were examined by unpaired Student's t-test.
CB, carbon black; AST, aspartate aminotransferase; ALT, alanine aminotransferase; 8-OHdG, 8-hydroxy-2'-deoxyguanosine; IL-6, interleukin-6; CRP, C-reactive protein; MCP-1, monocyte chemoattractant protein-1.

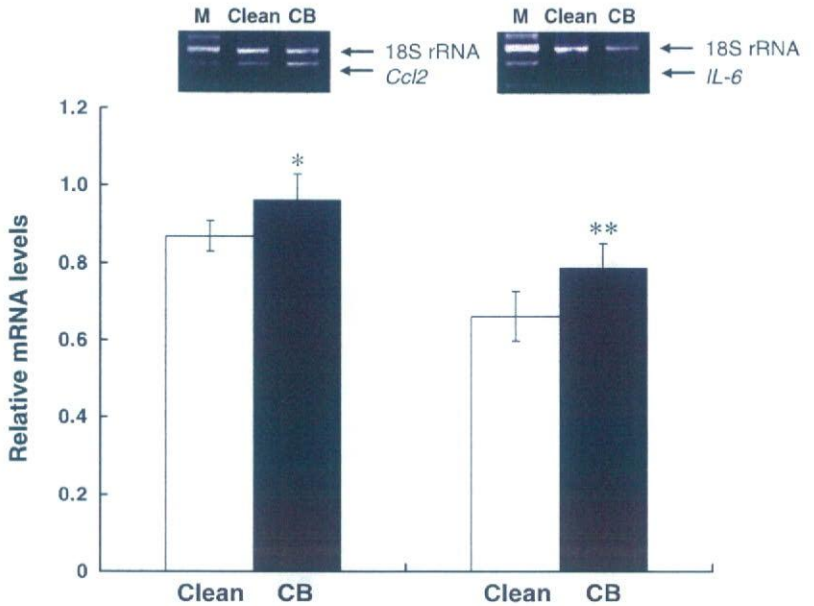

Fig 2. Expression levels of *Ccl2* and interleukin-6 (*IL-6*) mRNA in the lungs of carbon black (CB)-treated (n=4) and filtered-air treated (n=5) rats were compared by competitive RT-PCR with the use of 18S ribosomal RNA as an internal standard. The size of the PCR products for *Ccl2*, *IL-6* and 18S RNA was 381 bp, 346 bp, and 489 bp, respectively. Non-parametric tests revealed a statistically significant difference in the *Ccl2* and *IL-6* mRNA expression levels between the 2 groups; *p=0.05 and **p=0.0143. Representative PCR products are shown with a 100-bp DNA marker (M). Vertical bars indicate standard deviation.

Histology and Electron Microscopy

Lungs removed after 28 days of exposure were fixed in 4% paraformaldehyde-buffered solution (pH 7.4) overnight at 4°C and then placed in PBS-buffered solution (pH 7.4). The tissues were dissected from the left lobes between the lung bronchioles and alveolar lung, and the small tissues were embedded in paraffin. Sections of 1-μm thickness were stained with hematoxylin–eosin, Giemsa, and elastica van Gieson.

For electron microscopy, the lungs, liver, spleen and aorta from rats exposed for 14 days were used. After fixation for 1 h at 4°C in 0.1 mol/L sodium cacodylate buffer (pH 7.4) containing 2.0% glutaraldehyde, the tissues (lung, liver, spleen and aorta) were subjected to overnight post-fixation in 0.1 mol/L sodium cacodylate-buffer (pH7.4) with 1.0% osmium tetroxide at 4°C. After dehydration in an ethanol gradient (50–100% each for 10 min), samples were embedded in EPON812 at 60°C for 2 days. Ultrathin sections (80 nm) were stained with uranyl acetate and lead citrate. The sections were examined with an electron microscope (JEM2000X, JEOL Ltd, Tokyo, Japan) at 100 kV.

Analysis of mRNA Expression Levels of IL-6 and Ccl2 by Semi-Quantitative Competitive RT-PCR

Total RNA was extracted from the lung tissues of CB-treated (n=4) and air-treated rats (n=5) using Trizol reagent (Invitrogen, CA, USA) according to the manufacturer's instruction. Five micrograms of extracted total RNA were reverse transcribed using SuperScript II (Invitrogen, San Diego, CA, USA) and random primer (Takara-Bio, Shiga, Japan). No PCR product was detected when the reactions were carried out in the absence of reverse transcriptase. Levels of *IL-6* and *Ccl2* mRNA expression in the lung tissues were quantified using 18S ribosomal RNA as an internal standard (QuantumRNA 18S Internal Standards Kit, Ambion Inc, TX, USA) as previously described[18] The ratios of the 18S primers to 18S competimers were 1.5:8.5 for *Ccl2* and 1:9 for IL-6, respectively. Competitive PCR reactions were performed for each cDNA using the following sense and anti-sense primers; 5'-GAGTTCCGTTTCTACCTGGAGTTT-3' and 5'-CAGGATATATTTTCTGACCACAGTGAG-3' for *IL-6*, and 5'-CAGGTCTCTGTCACGCTTCTG-3' and 5'-GTGGAAAAGAGAGTGGATGCAT-3' for

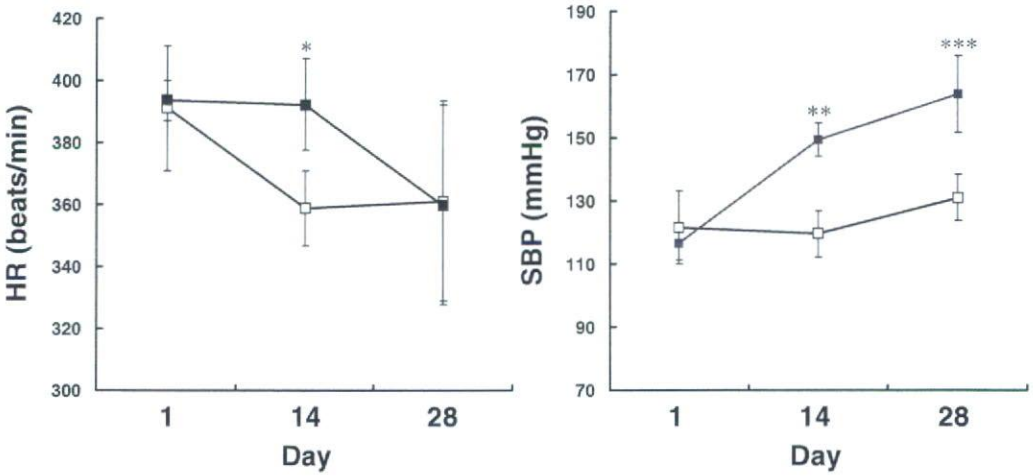

Fig 3. Effect of whole-body inhalation exposure of carbon black (CB) on heart rate (HR) and blood pressure (BP), which were measured by tail-cuff plethysmography after 1, 14, and 28 days of exposure. Each point represents a group of 3 rats. (Open squares) Control group (n=3), (filled squares) CB-treated group (n=3). Although HR measured on days 1 and 28 did not differ between the control and CB groups, HR on day 14 was significantly elevated in the CB group compared with the control group. In rats exposed to CB, levels of systolic BP (SBP) increased in an exposure-time dependent manner. Asterisks denote significant differences between the groups: *p=0.0383, **p=0.0046, and ***p=0.0164. Vertical bars indicate standard deviation.

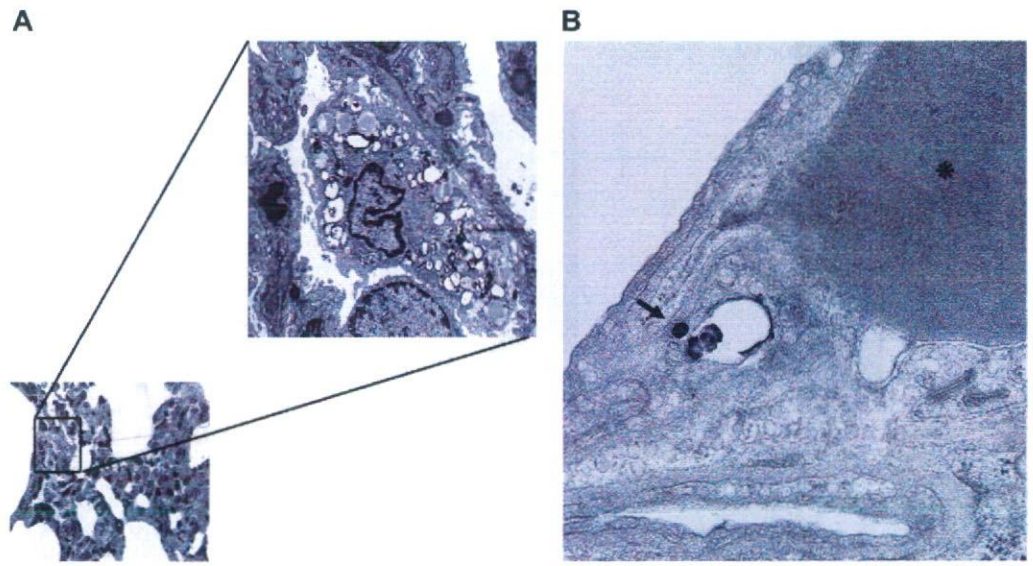

Fig 4. Representative electron micrograph of alveolar tissue in rats exposed to carbon black (CB) for 14 days shows CB in macrophage-like cells (A, ×2,500). CB is also seen in endothelial cells of a blood capillary (B, ×10,000). Arrow indicates a CB compartment in an autophagic-like structure in the endothelial cell. *Red blood cells.

Ccl2. The intensities of the PCR products from the *Ccl2* (381 bp) and *IL-6* (346 bp) mRNA relative to those from 18S RNA (489 bp) were assessed by densitometry. Results are expressed as arbitrary units.

Statistical Analysis

Results are expressed as mean ± SD. Differences in hematological and biochemical parameters between the CB-treated and filtered air-treated control groups were examined by 2-tailed unpaired Student's t-test. Differences in BP and HR measured at day 1, 14 and 28 (n=3 for each group at each point) were compared between the CB and control groups using a 2-tailed unpaired Student's t-test. Because of the non-normal distribution and semi-quantitative nature of RT-PCR, the non-parametric Wilcoxon/Kruskal-Wallis test was used for comparisons of the mRNA expression levels between the CB-treated and filtered air-treated control groups. Statistical analysis was performed using the JMP statistical package 6.0 (SAS Institute, Cary, NC, USA). P-values <0.05 were considered statistically significant.

Results

There were no differences between the CB and control groups in baseline body weight, and the time-course increase in body weight was not different between the 2 groups (data

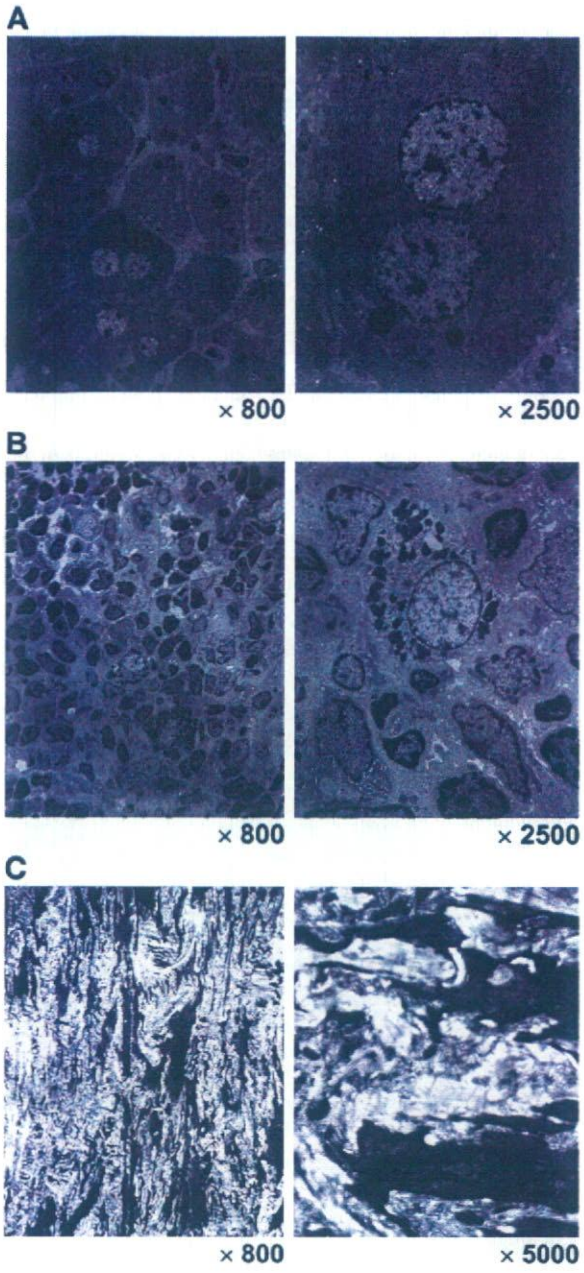

Fig 5. Representative electron micrographs of liver, spleen and aortic endothelial cells of carbon black (CB)-exposed rats. CB particles are not seen in (A) the liver sections (Left, ×800; Right, ×2,500), (B) the spleen (Left, ×800; Right, ×2.500) or (C) the endothelial cells (Left, ×800; Right, ×5,000).

not shown). Hematological and biochemical parameters measured on day 28 or 30 day were compared between the CB and control groups (Table 1). No significant differences were observed between the groups for the number of red blood cells, white blood cells or platelets. Plasma levels of alanine aminotransferase (ALT) and aspartate aminotransferase (AST), often used as markers of liver injury, did not differ between the groups. There was no effect of CB inhalation on serum albumin, creatinine, creatine kinase, and 8-OHdG levels. Circulating levels of MCP-1 and CRP were significantly elevated in rats exposed to CB for 4 weeks ($p=0.0024$ and $p=0.0003$, respectively). IL-6 tended to be increased in the CB group compared with the control group ($p=0.05$). In accordance with this observation, higher expression levels of *IL-6* and *Ccl2* mRNA were observed in the lungs of rats exposed to CB for 28 days than in those of controls (Fig 2).

Although there was no difference between the control and CB groups in HR measured on days 1 and 28, HR was significantly elevated in the CB group compared with the control group after 14 days of inhalation of CB (Fig 3). CB exposure significantly raised systolic BP (SBP) levels, with the CB group having a significantly higher SBP on days 14 and 28 compared with controls (Fig 3).

Electron microscopic examinations revealed the presence of CB in macrophage-like cells and endothelial cells in blood capillaries deep in the lungs (Figs 4A,B). Most of the CB particles were located in phagosome-like structures in the cytoplasm of alveolar macrophages. CB was not detected in the liver, spleen or endothelial cells from the abdominal aorta (Fig 5). Examination of pulmonary tissues stained with hematoxylin–eosin, Giemsa, and elastica van Gieson showed no difference in the staining pattern between the CB and control groups, with no signs of alveolar destruction or fibrosis in the CB group (data not shown).

Discussion

One of the purposes of the present study was to clarify whether whole-body exposure of CB might result in translocation of the particles into the systemic circulation, eventually reaching the extrapulmonary tissues. Although it has been previously reported that nanoparticles are able to penetrate into the deep lung areas and pass through to reach the systemic circulation[14] we did not observe any CB signals in extrapulmonary tissues, including the liver, spleen and aorta, by electron-microscopic examination. This is in agreement with our recent report showing the absence of CB particles in the liver, aorta, kidney and spleens of LDLR/KO mice exposed to CB for 10 weeks by intra-tracheal administration[11]

In the present study, rats were exposed to CB for 6 h/day, 5 days a week for a total of 4 weeks at nominal concentrations of $15.6\pm3.5\,mg/m^3$, with a median particle diameter of 116.4 nm. According to the air-pollution data collected in the urban areas of China[19] mean and maximum concentrations of particulate matter less than $2.5\,\mu m$ in diameter have been reported to be 146.8 and $666.2\,\mu g/m^3$, respectively. The dosage used in the present analysis is approximately 20- to 100-fold higher than the ambient air pollution in China. Despite the higher dosage and different method of exposure used in our present analysis, we could not confirm the translocation of inhaled carbon nanoparticles into the bloodstream or other tissues. In line with these findings, 4-week exposure to CB did not have any significant effect on liver and renal functions as assessed by ALT, AST, creatinine and creatine kinase. Thus, nano-sized CB particles are likely to aggregate in the lung, and are unlikely to pass through the alveoli and exert direct toxic effects on other target tissues.

What is clear from our present study is that exposure to CB by inhalation induced incorporation of CB in pulmonary macrophages in SD rats. Electron microscopic examination revealed the existence of CB particles in autophagic-like cellular structures of pulmonary endothelial cells of the capillary vessels of CB-treated rats. Circulating levels of

MCP-1, IL-6 and CRP, known as inflammatory marker proteins, were markedly elevated in rats exposed to CB for 4 weeks compared with the controls. Although a severe form of alveolar inflammation or fibrosis was not observed in rats exposed to CB, it is certain that CB exposure induced a mild inflammatory response in the lung. Exposure to diesel exhaust particles has been reported to induce the release of proinflammatory cytokines, such as IL-1β and IL-8, in human bronchial epithelial cells[20,21] A study examining the effect of silica exposure on the production of inflammatory mediators in the lung has shown upregulation of *IL-6* and *MCP-1* in alveolar macrophages and fibroblasts[22] Therefore, in the present study the increased levels of *Ccl2* and *IL-6* mRNA expression in the lungs of CB-treated rats may account for the differences in the circulating levels of IL-6 and MCP-1 between the 2 groups. Cytokines associated with inflammation are known to trigger the production of acute-phase proteins, with IL-6 being the major stimulator of CRP synthesis in the liver[23] Local production of IL-6 may be responsible for a rise in CRP. Our results may support the hypothesis that a mild inflammatory response elicited in the lung by deposition of inhaled particulate matter leads to atherothrombotic diseases[12]

It is noteworthy that exposure to CB raised SBP in an exposure-time dependent manner. Although there was no difference between the CB and control groups in HR measured at the end of 4-week exposure, rats exposed to CB had a significantly higher HR at day 14 after exposure. Associations between ambient air pollution and elevated BP have been documented in humans[5–8] Although the retrospective analysis of the Augsburg MONICA surveys (1984–1985/1987–1988) did not have detailed data on the concentrations of nano-sized particles, an effect of total suspended particulates on SBP was demonstrated, with greater effects being observed among the subgroups with high plasma viscosity and elevated HR[5] The exact mechanisms of how CB exposure leads to higher BP await further investigation, but may involve activation of the sympathetic nervous system by the inflammatory response and/or respiratory distress because of the accumulation of CB particles in the lungs.

Although the method of CB exposure was improved from the intra-tracheal dispersion used in our previous report to whole-body inhalation in the present study, we found no evidence of the translocation of inhaled nano-sized particles to the circulation or extrapulmonary tissues. Thus, the possibility of a direct, deleterious effect of nano-sized particles on endothelial cells or extrapulmonary tissues can be considered minimal. Although the question of whether a trace amount of CB particles penetrated into the systemic circulation, but was not detected in ultrathin sections and caused toxic effects remains unanswered, we have confirmed that relatively high concentrations of CB particles are necessary to damage cells in vitro![6] Thus, the association between cardiovascular risk and air pollution is more likely to be explained by the inflammatory response induced by the accumulation of inhaled nano-sized particles in the deep lung. Determination of safety levels of particulate matter in the air from the viewpoint of health hazard is warranted.

Acknowledgments

The authors would like to thank Fumio Ichinose and Masafumi Horiuchi of CERI for their technical support with the CB exposure.

The present study was supported by the Health and Labor Science Research Grant: Research on Risk of Chemical Substance (H17-Chemistry-008).

References

1. Zanobetti A, Canner MJ, Stone PH, Schwartz J, Sher D, Eagan-Bengston E, et al. Ambient pollution and blood pressure in cardiac rehabilitation patients. *Circulation* 2004; **110:** 2184–2189.
2. Brook RD, Franklin B, Cascio W, Hong Y, Howard G, Lipsett M, et al. Air pollution and cardiovascular disease: A statement for healthcare professionals from the Expert Panel on Population and Prevention Science of the American Heart Association. *Circulation* 2004; **109:** 2655–2671.
3. Sun Q, Wang A, Jin X, Natanzon A, Duquaine D, Brook RD, et al. Long-term air pollution exposure and acceleration of atherosclerosis and vascular inflammation in an animal model. *JAMA* 2005; **294:** 3003–3010.
4. Suwa T, Hogg JC, Quinlan KB, Ohgami A, Vincent R, van Eeden SF. Particulate air pollution induces progression of atherosclerosis. *J Am Coll Cardiol* 2002; **39:** 935–942.
5. Ibald-Mulli A, Stieber J, Wichmann HE, Koenig W, Peters A. Effects of air pollution on blood pressure: A population-based approach. *Am J Public Health* 2001; **91:** 571–577.
6. Linn WS, Gong H Jr, Clark KW, Anderson KR. Day-to-day particulate exposures and health changes in Los Angeles area residents with severe lung disease. *J Air Waste Manag Assoc* 1999; **49:** 108–115.
7. Linn WS, Gong H Jr. Air pollution, weather stress, and blood pressure. *Am J Public Health* 2001; **91:** 1345–1346.
8. Urch B, Silverman F, Corey P, Brook JR, Lukic KZ, Rajagopalan S, et al. Acute blood pressure responses in healthy adults during controlled air pollution exposures. *Environ Health Perspect* 2005; **113:** 1052–1055.
9. Pope CA 3rd, Verrier RL, Lovett EG, Larson AC, Raizenne ME, Kanner RE, et al. Heart rate variability associated with particulate air pollution. *Am Heart J* 1999; **138:** 890–899.
10. Erdogmus B, Yazici B, Annakkaya AN, Bilgin C, Safak AA, Arbak P, et al. Intima-media thickness of the common carotid artery in highway toll collectors. *J Clin Ultrasound* 2006; **34:** 430–433.
11. Niwa Y, Hiura Y, Murayama T, Yokode M, Iwai N. Nano-sized carbon black exposure exacerbates atherosclerosis in LDL receptor knock-out mice. *Circ J* 2007; **71:** 1157–1161.
12. Seaton A, MacNee W, Donaldson K, Godden D. Particulate air pollution and acute health effects. *Lancet* 1995; **345:** 176–178.
13. Donaldson K, Stone V, Seaton A, MacNee W. Ambient particle inhalation and the cardiovascular system: Potential mechanisms. *Environ Health Perspect* 2001; **109**(Suppl 4): 523–527.
14. Nemmar A, Hoet PH, Vanquickenborne B, Dinsdale D, Thomeer M, Hoylaerts MF, et al. Passage of inhaled particles into the blood circulation in humans. *Circulation* 2002; **105:** 411–414.
15. Niwa Y, Iwai N. Nanomaterials induce oxidized low-density lipoprotein cellular uptake in macrophages and platelet aggregation. *Circ J* 2007; **71:** 437–444.
16. Yamawaki H, Iwai N. Mechanisms underlying nano-sized air-pollution-mediated progression of atherosclerosis: Carbon black causes cytotoxic injury/inflammation and inhibits cell growth in vascular endothelial cells. *Circ J* 2006; **70:** 129–140.
17. Yamawaki H, Iwai N. Cytotoxicity of water-soluble fullerene in vascular endothelial cells. *Am J Physiol Cell Physiol* 2006; **290:** C1495–C1502.
18. Iwai N, Yasui N, Naraba H, Tago N, Yamawaki H, Sumiya H. Klk1 as one of the genes contributing to hypertension in Dahl salt-sensitive rat. *Hypertension* 2005; **45:** 947–953.
19. Venners SA, Wang B, Xu Z, Schlatter Y, Wang L, Xu X. Particulate matter, sulfur dioxide, and daily mortality in Chongqing, China. *Environ Health Perspect* 2003; **111:** 562–567.
20. Bayram H, Devalia JL, Sapsford RJ, Ohtoshi T, Miyabara Y, Sagai M, et al. The effect of diesel exhaust particles on cell function and release of inflammatory mediators from human bronchial epithelial cells in vitro. *Am J Respir Cell Mol Biol* 1998; **18:** 441–448.
21. Boland S, Baeza-Squiban A, Fournier T, Houcine O, Gendron MC, Chevrier M, et al. Diesel exhaust particles are taken up by human airway epithelial cells in vitro and alter cytokine production. *Am J Physiol* 1999; **276:** L604–L613.
22. Rao KM, Porter DW, Meighan T, Castranova V. The sources of inflammatory mediators in the lung after silica exposure. *Environ Health Perspect* 2004; **112:** 1679–1686.
23. Gabay C, Kushner I. Acute-phase proteins and other systemic responses to inflammation. *N Engl J Med* 1999; **340:** 448–454.